Electron-atom Collision Cross Sections in Argon: An Analysis and Comments

Gorur G. Raju
Department of Electrical and Computer Engineering
University of Windsor
Windsor, Ontario, N9B 3P4, Canada

ABSTRACT

Experimental data on electron-atom collision cross sections in argon published during the period 1980-2002 are compiled and reviewed, with 123 references. Total, integral elastic, differential, excitation and ionization cross sections in the energy range 0–1000 eV are considered separately. A comparison between various measurements and, between various semi-empirical formulas are given. Improved formulas previously unpublished are also given where required. The sigma rule (the total cross section is the sum of partial cross sections) holds good in argon to an accuracy of $\pm 5\%$ in the energy range 12–1000 eV. A recommended set is provided.

Index Terms — **Cross sections, collisions, electrical discharges, beam experiments, rare gases, argon, integral elastic cross section, differential cross section, excitation cross section, ionization cross section.**

1 INTRODUCTION

ELECTRON molecule collision cross sections are important in a number of areas that deal with discharges, plasma chemistry, fusion research, solution of the Boltzmann equation, Monte Carlo simulation, swarm experiments etc. [1]. Data on cross sections are one of the most fundamental in the study of gaseous electronics and beginning with the measurements of Ramsauer [2] and Brode [3], a large number of measurements have been carried out in several gases and a summary of these early investigations are given by Massey and Burhop [4], Bederson and Kieffer [5], Brandsen and McDowell [6] and in books by McDaniel [7] and Hasted [8]. A thorough summary of data till the year 1994 is published by Trajmar and McKonkey [9] and Zecca et. al. [10]. In view of the central role which these data play in all facets of gas discharges and plasma science, it is felt that an analysis of measured data is timely mainly for use by the engineering community, and others in the areas of plasma science technology.

This paper makes such an analysis in argon with comments aimed at helping choice of data for an intended purpose. In view of the references quoted above, papers published after 1980 are considered unless earlier references are required to maintain continuity. To limit the scope of treatment, theoretical papers are not considered in detail, though some papers are referred to, due to the fact that they are part of a figure in the presentation of experimental data. The paper also contains previously unpublished expressions for ionization cross sections in addition to, calculations of differences of cross sections obtained by different methods and semiempirical equations.

Argon gas has been studied from the discharge point of view for more than 100 years and interest in this gas is due to several important fundamental and technical considerations. Its presence in high concentrations plays a major role in the performance of the high pressure Ar-Kr-F_2 laser system and in direct nuclear-pumped lasing media using He-Ar mixtures, Chutjian and Cartwright [11].

Argon gas has been subjected to intense study since the discovery of a minimum at low electron energies by Ramsauer [12, 13] and, Townsend and Bailey [14, 15]. Easy availability of the gas and the interest aroused by the successful explanation of the effect by the application of the quantum mechanical method [16] added further interest. We summarize the data obtained during the past thirty years or so. Table 1 shows selected references for cross section measurements in argon in chronological order and as an aid to follow the references listed at the end of the chapter. It is convenient to include other rare gases as well in this table, as several of these gases are usually measured by the same group using the same apparatus. Further, a second paper is being completed in the remaining rare gases and Table 1 is intended to serve as a reference for the follow up paper as well. In order to assist the

Manuscript received on 20 February 2003, in final form 22 September 2003.

reader in reading the text brief definitions and brief experimental techniques are included in the next section.

An attempt to provide a relative agreement between several methods and several groups is beset with the problem of choosing a reference cross section. Each group of authors generally chooses own values against which other measurements are compared. A compilation of these results, therefore, necessarily involves an arbitrary choice of reference and analytical formulations are convenient to use in such circumstances. Values of cross sections provided by analytical equations, by Brusa et al. [17] and Zecca et. al. [18] for example, cover a broad range of electron energies and provide a convenient base for comparison.

A few remarks about the analytical equations for expressing the cross sections as a function of electron energy are in order. A number of equations are available in the literature for representing various cross sections and, as noted by Inokuti et al. [19], these expressions have a theoretical basis and have adjustment parameters, appropriate to each gas. Such equations are useful in the presentation of data of a large number of gases, as otherwise one has to resort to extensive tables that are not the most efficient way of presenting data, particularly if a large energy range of energies covering several decades is involved.

Further, the analytical equations are helpful to evaluate quickly the cross sections at a given energy, particularly in situations where repeated reference to closely spaced electron energies are required. Boltzmann equation analysis and Monte Carlo simulations are examples of such requirement. The functions for cross sections will not, of course, have a perfect agreement with measurements and the discrepancy between individual sets of measurements and the values obtained by the analytical functions should be made available. Since the experimenters do not always choose the same energy steps for measurement of cross sections, analytical expressions are valuable to calculate the cross sections at odd values of the electron impact energy. The user can then determine the degree of accuracy required for a specific application and choose the data that satisfy this requirement.

The analytical functions for elastic scattering of electrons are useful to find the zero energy cross section $Q(\epsilon = 0)$, by extrapolation. This quantity is equated to $4\pi A^2$ where A has the dimension of length and is known as the scattering length. It appears in the expression for s-wave scattering shifts in the quantum mechanical description of the collision phenomena [20] providing a link between theory and the analytical function. The relation of the analytical functions to the theory has been discussed by Inokuti et. al. [21] and the types of functions useful to represent several different cross sections are also provided by them. The generally accepted analytical functions for the collision cross sections are based on the

Table 1. Selected references for collision cross section data in rare gases. Q_T = Total, Q_M = Momentum transfer, Q_{el} = Elastic, Q_{dif} = Differential, Q_{ex} = Excitation, $Q_{ex,\ T}$ = Total excitation, Q_{Met} = Metastable, Q_i = ionization, $Q_{in,\ T}$ = Total inelastic, Q (set) = Complete set. H = magnetic field, EI = electron impact, PE = Photoelectron, MS = Mass spectrometer.

Type	Gas	Energy range (eV)	Method	Source
Q_T	Ar, He,	0.1−100	Direct beam	Brode [3] (1925, 1933, 1942).
Q_{dif}	Ar, Kr, Xe	0.6−12.5	Direct beam	Ramsauer et al. [13] (1932)
Q_i	Ar, He, Ne, Kr, Xe	ϵ_i−100 eV	Beam-static gas	Asundi et al. [90] (1963)
Q_M	Ar	0-20	Swarm coefficients	Engelhardt et al. [62] (1962)
Q_i	Rare gases	–	Review	Kieffer et al. [84] (1966)
Q_i	Ar, He, Ne,	$\epsilon_i - 1000$	Beam-static-gas	Rapp et al., [85] (1965).
Q_T	Ar, He	0.1−20	Ramsauer method	Golden et al. [27] (1965, 1966).
Q_i	Ar, He, Kr, Ne, Xe	0.5k-18k eV	Ionization tube/Mass spectrometer	Schram et al. [91] (1965, 1966).
Q_i	He, Ar	onset-500	beam-static-gas	Fletcher et al. [102] (1973)
Q_{ex}	Ar	20-2000	Crossed beam	McConkey et al. [32] (1973)
Q_T	He	1-50	Time of Flight	Kennerly et al. [36] (1978).
Q_{el}, Q_T, Q_{ex}	Ar, Kr, Ne, Xe	20-3000	Semi empirical	de Heer et al. [55] (1979)
Q_{dif}	Ar, He, Ne,	0.5-20 eV	Crossed beam	Williams [69] (1979)
Q_T	He	100-1400	Modified Ramsauer	Dalba et al. [28] (1979)
Q_T	Ar, He	500-5000	beam-static gas	Nagy et al. [96] (1980)
Q_T	Ar, Ne, Kr	25-750	Transmission	Wagenaar et al. [58] (1980)
Q_i	Ar, He, Ne, Kr	Onset-200	Mass spectrometer	Stephan et al. [87] (1980)
Q_{ex}	Ar	16-100	Crossed beam	Chutjian et al. [11] (1981).
Q_i	He	25-2000	Modified Ramsauer	Dalba et al. [29] (1981)
Q_M, Q_{dif}	Ar, Kr	3-100	Crossed beam	Srivastava et al. [60] (1981)
Q_T	Ar, He, Ne	15-800	Transmission employs **H.**	Kauppila et al. [56] (1981)
Q_{diff}	Ar, Kr	10-50	Crossed beam	Zhou King et al. [45] (1982)
Q_T	Ar	500-3000	Transmission with **H**	Nogueira [59] (1982)
Q_T	Ar, Kr, Xe,	0.05-60	Transmission	Jost et al. [34] (1983)
Q_i	Ar, Kr	onset-150	Mass spectrometer	Mathur et al. [53] (1984, 1986)
Q_d, Q_M,	Ne	1-100	Crossed beam	Register et al. [46] (1984)

 1070-9878/04/$20.00 © 2004 IEEE

Table 1 (Contd.)

Type	Gas	Energy range (eV)	Method	Source
Q_T	Ar, He, Ne, Xe, Ar	4-300	Linear transmission	Nickel et al. [33] (1985)
Q_T		0.08-20	Time of flight, employs **H.**	Ferch et al. [37] (1985)
Q_T	Ar, Kr, Xe	20-100	Transmission	Wagenaar et al. [34] (1985)
Q_T	Ar, He	0.12-20	Time of flight	Buckman et al. [38] (1986)
Q_T	Ar, Kr and Ne	700-6000	Linear transmission	Garcia et al. [26] (1986)
Q_{dif}	Ar, He, Ne, Kr	20-200	Linear transmission	Wagenaar et al. [35] (1986)
Q_{dif}, Q_{el}, Q_M	Ar	300-1000	Crossed beam with **H**	Iga et al. [47] (1987)
Q_{Met}	Ar	12-142	Time of flight	Mason et al. [39] (1987)
Q_M, Q_{el}	Ar	3-300	Theory	Nahar et al. [63] (1987)
Q_i	Ar, He, Ne, Kr	0-200	Fast neutral beam	Wetzel et al. [50] (1987)
Q_T	Ar, Kr, Xe	0.7−10	PE spectroscopy	Subramanian et al. [59] (1987)
Q_T	Ar, Ne	100-3000	Modified Ramsauer	Zecca et al. [30] (1987)
Q_{i1}, Q_{i2}	He	26.6−10000	Pulsed crossed beam	Shah et al. [51] (1988)
Q_i	Ar, He, Kr, Ne, Xe	ϵ_i-1000	Pulsed electron beam mass spectrometer	Krishnakumar et al. [52] (1988)
Q_i	Ar, He, Kr, Ne, Xe	ϵ_i-10000	Review	Lennon et al. [89] (1988)
Q_{diff}	Ar	0.05-2	Mass spectrometer	Weyhreter et al. [65] (1988)
Q_T & Q_{dif}	Ar	3-20	Time of flight	Furst et al. [40] (1989)
Q_T	Kr, Xe	80-4000	Modified Ramsauer	Zecca et al. [31] (1991)
Q_i	Ar^+, Ar^{2+}, Ar^{3+}	20-100	Time of flight MS	Bruce et al. [98] (1992)
Q_i	Ar^+, Ar^{2+}, Ar^{3+}	20-100	Time of flight MS	Ma et al. [97] (1991)
Q_M	Ar, He, Kr, Xe	0.001-100	Swarm analysis	Pack et al. [60] (1992)
Q_i	Kr and Xe	0-470 eV	Time of flight	Syage [41] (1992)
Q_i	Ar^+ to Ar^{5+}	18-5300	Time of flight	McCallion et al. [42] (1992)
Q_{ex}	Ar, Kr, Xe	onset-60	Optical absorption	Mityureva et al. [80] (1994)
Q_i	Ar	onset-1000	Time of flight	Straub et al. [103] (1995)
Q_{dif}, Q_{el}, Q_M	Ar	1-10	Crossed beam	Gibson et al. [49] (1996)
Q_{ex}	Ar	11-1000	Photon counting	Tsurubuchi et al. [81] (1996)
Q_{dif}	Ar	10	Spectrometer	Zubek et al. [66] (1996)
Q (set)	–	0.001-1000	Compilation	Pitchford et al. [83] (1996)
Q_T, Q_{ex}, Q_i	Ar, Ne, Kr, Xe	10-10000	Semiempirical	Brusa et al. [17] (1996) For a correction see Zecca et al. [18] (2000).
Q_{dif}	Ar, Kr	20-235	EI spectrometer	Cvejanović and Crowe [67] (1997)
Q_{dif}	Ar	10-100	Crossed beam	Panajotović et al. [71] (1997)
Q_{dif}	Ar, He, Kr, Ne, Xe		Spectrometer	Zubek et al. [104] (1999)
Q_m, Q_{ex}, Q_i	Ar	–	Semiempirical	Phelps et al.[100] (1999).
Q_i	Ar, Kr, Xe	140-1000	Electron beam	Sorokin et al. [86] (2000)
Q_{ex}	Ar	20-80	EI spectrometer	Filipović et al. [76] (2000)
Q_{ex}	Ar	20-80	EI Spectrometer	Filipović et al. [82] (2000)
Q_T	Ar, Ne, Kr, Xe	0.5 eV-10 keV	Semi-empirical	Zecca et al. [18] (2000)
Q_{dif}	Ar	10.3-160.3	Theory	Sienkiewicz et al. [72] (2001)
Q_i	Ar, Ne, Kr, Xe	onset-1000	Time of flight	Kobayashi et al. [99] (2002)

Born-Bethe approximation, with some fitting parameters for each gas. This procedure has been found to be more applicable in the high energy range, > 500 eV.

Zecca et. al. [22, 23, 24], March et al. [25], Garcia et. al. [26] and Brusa et al. [17] have, however, generated functions for molecular and rare gases, respectively and the expressions are easy to use. One has to bear in mind that evaluation of the fitting parameters involves choosing data from one or few groups, thereby indirectly bestowing them the status of reference values because all other measurements are compared to the selected data. However on the basis of stated accuracy of the measurements and the close agreement between the results of several groups renders the procedure justifiable. We adopt the procedure of Zecca et al. [10] in presenting data; however, the required number of decades are chosen in preference to their two decades, and a percent difference graph is added for each cross section as calculated from the tabulated values in the original reference.

2 DEFINITIONS OF CROSS SECTIONS

Collisions between electrons and neutrals are of three kinds; (1) elastic collisions in which the total kinetic energy of the colliding particles remains the same and there is an exchange of momentum. (2) Inelastic collisions in

which part of the kinetic energy of one particle goes into changing the internal energy of the other particle. Excitation and ionization are the most frequently encountered inelastic collisions in rare gas atoms. In molecular gases the vibrational and rotational cross sections that occur at low electron energies are also inelastic collisions. (3) Superelastic collisions or the collision of the second kind in which the internal energy is converted into kinetic energy. The following notations are used.

1. Q_M: Momentum transfer cross section.

2. Q_{el}: Elastic collision cross section, also referred to as elastic integral cross section.

3. Q_{diff}: Differential cross section is defined as

$$Q_{el} = 2\pi \int_0^{\pi} Q_{diff}(\theta) \sin\theta \, d\theta \tag{1}$$

where θ is the scattering angle of the electron after a collision occurs. The definition of equation (1) is not limited to elastic collisions. Vibrational excitation, momentum transfer and excitation cross sections have their respective differential scattering given by

$$Q_{\upsilon} = 2\pi \int_0^{\pi} Q_{\upsilon,\,diff} \sin\theta \, d\theta \tag{2}$$

$$Q_M = 2\pi \int Q_{el,\,diff} \sin\theta \, (1-\cos\theta) \, d\theta \tag{3}$$

$$Q_{ex} = 2\pi \int_0^{\pi} Q_{ex,\,diff} \sin\theta \, d\theta \tag{4}$$

In equations (1)–(4) the respective differential cross sections are measured and corresponding collision cross sections are obtained by integration.

4. Q_{ex}: Excitation cross section inclusive of metastable levels.

5. Q_i: Ionization cross section.

6. Q_T: The total cross section which is the sum of all collision cross sections,

$$Q_T = \Sigma Q_{elas} + \Sigma Q_{inelas} \tag{5}$$

The collision cross sections in the literature are expressed in units of m^2, $a_o^2 = 0.28 \times 10^{-20}$ m^2, $\pi a_o^2 = 0.88 \times 10^{-20}$ m^2 or $Mb = 10^{-22}$ m^2. We use units of m^2 throughout.

3 EXPERIMENTAL METHODS

This paper is not meant to discuss the various experimental techniques that have been developed to measure the cross sections. However, to understand the text in the following sections better, a brief description is provided. Basically, measurements of cross sections fall into two broad categories: 1) transmission method. A parallel or perpendicular magnetic field is employed as also a nonmagnetic field. The cross section is measured by employing the Beer-Lambert law

$$I = I_o \exp(-Q_T nL) \tag{6}$$

where I is the current measured, I_o is the current in the absence of scattering (in vacuum), n the gas number density and L the scattering length. A source of error in this technique is the contribution of the forward scattered electrons, to the transmitted current leading to incorrect cross sections. This consideration will be commented upon later. 2) Crossed beam method. A beam of electrons intersects a beam of atoms effusing from a set of capillary nozzles. This method is the preferred, but not exclusive, method for measuring the excitation and ionization cross sections.

The transmission method employing a perpendicular magnetic field may be grouped as under:

1. The Ramsauer method [2, 12, 27] for total cross section measurements: In this technique a beam of electrons having a well-defined energy is allowed to interact with neutrals. A perpendicular magnetic field is meant to serve two purposes: energy selection and enhanced angular resolution. The number of electrons that survive collision is measured by directing them to a collecting chamber, as also the number of electrons in the beam before collision. The ratio of numbers of electrons or currents is used to obtain the cross section.

The Ramsauer technique adopts the technique of electron energy selection by the application of the magnetic field perpendicular to the orbital plane. Although this technique is basically simple, it is difficult to control the spread of the electron beam precisely. The detector registers an unknown number of such electrons, thus reducing the absorption measured. This source of error lowers the measured total cross section.

2. Modified Ramsauer technique [28–31] for total cross section. In the Ramsauer technique electrons that are scattered by a small angle are also collected by the collector resulting in erroneous value of the cross section. In the modified method the collision chamber is divided into two sections, one section being at a higher pressure than the other. The electrons collected scattered through a small angle do not make a contribution to the measurement, resulting in improved accuracy [29].

The transmission method without a magnetic field may be grouped as under:

3. The linear transmission method [26, 32–35]: Use of magnetic fields in the Ramsauer-Townsend method is a distinct disadvantage from the point of view of number of parameters to control. The linear transmission method dispenses with the magnetic field. Electrons of known energy are transmitted through the scattering chamber and those electrons that survive collision are detected. The method, again, gives the total collision cross section.

4. The time of flight method [36–42] uses a pulse of electrons and measures the time of arrival of the electrons at the collecting electrode. Time to amplitude conversion of the signal is involved. A comparison is made of the

signal that is obtained in the presence and absence of target atoms to determine the total cross section.

Transmission methods are subject to a systematic error as recognized by several authors because the transmitted current does not distinguish between the electrons scattered through a small angle. This effect results in an underestimation of the total cross section and the magnitude of the error increases with the electron energy.

5. Elastic collision cross section measurements, in fact, are differential cross section measurements and integrated according to the definition given previously. Differential cross section measurements involve collecting the electrons scattered through a small angle and varying the angle of the detector with respect to the beam axis. The angular resolution, defined by the aperture in front of the detector system, can be better than 0.2° and the angle reading better than 0.05°. As large an angle as possible is swept by the detector, in the range of 0 to π, to improve accuracy. Practical considerations preclude covering the entire range. For integration purpose the differential cross section should be extrapolated to 0° at one end and 180° at the other, adding to the uncertainty in the measurement. Recent advances have overcome this difficulty [43, 44] though for accuracy sake it is stated that the measured cross sections are due to electronic excitation in helium.

Differential cross section measurements [13, 45-47]: Ramsauer used a collector that was split into a number of segments and the cross section for scattering is measured as a function of the angle of scattering. In modern techniques either the electron gun or the detector is allowed to rotate for measuring the angular scattering cross section.

6. The modern techniques for the measurement of cross sections are of the crossed beam type, in which electrons interact with a stream of neutrals, effusing from a thin (~ 50 μm) capillary, at 90° to the beam. The technique is employed for measuring different cross sections, such as total [48], elastic [47, 49], excitation [32] and ionization [50-52]. While the principle is quite simple, as in many techniques of cross section measurements, ensuring accuracy demands experience and attention to details.

7. Ionization cross sections were measured, till about 1965, by the ionization tube method [25, 28, 30, 31] in which a nearly monoenergetic beam of electrons ionized the neutrals and the ion current is measured. Since the gas pressures employed are of the order of 10^{-2} Pa the ratios of charge carriers to neutrals reach an unacceptably high value and it is necessary to replenish the gas. The number of ions formed is proportional to the pressure, and the fractional error in pressure caused by ion pumping is independent of gas pressure provided that the mean free path is long. Target gas is replenished by pumping the ionizing chamber differentially through a minute orifice and feeding the experimental gas through a needle valve. Though the gas is continuously replenished these experiments are classified as beam-static gas type.

8. Recent techniques involve the crossed beam configuration [50], with the electron beam being pulsed [51, 52] and the time of flight method is applied to the signal. Mass spectrometer [47, 53] is used to measure partial ionization cross sections.

9. The difficulties associated with the accurate determination of the gas number densities for the determination of the absolute ionization cross sections has given rise to innovative ideas. Photoelectron yields are compared with the electron impact yield of ions, measured in the same ionization tube. Since the former is known to an uncertainty of 2–3% [54], electron impact cross sections are determined with greater accuracy.

4 TOTAL AND MOMENTUM TRANSFER CROSS SECTIONS ($15 \leq \epsilon \leq 1000$ eV)

As mentioned earlier, we resort to semiempirical equation [17, 18], as reference, for comparison of the results of various investigators. The significance of the energy range considered is that it is to the right side of the maximum of the $\epsilon - Q_T$ curve and the empirical formulas are applicable for $\epsilon > 15$ eV.

De Heer et al. [55] calculated the total cross sections in argon in the energy range ($20 \leq \epsilon \leq 3000$ eV) by consideration of experimental and theoretical data available till then and their method is usually referred to as semi-empirical in the literature. Their tabulated data were employed by Zecca et al. [30] to evaluate a sixth order double logarithmic dependence of the total cross section on energy (i.e., $\log Q_T - \log \epsilon$) in the energy range ($100 \leq \epsilon \leq 3000$ eV); The resulting coefficients in order of ascending power of ϵ are: 0.67324, 0.75806, -0.25355, -0.105097, 0.04759, -0.00522 and -0.00006. The calculated values agree with the measured cross sections within $\pm 10\%$. A more recent function is due to Brusa et al. [17] in the energy range, $14 \leq \epsilon \leq 3000$ eV, as

$$Q_T = \frac{1}{A(B+\epsilon)} + \frac{1}{C_E} \tag{7}$$

in which A, B and C are fitting parameters and ϵ is the electron energy in keV. The parameters and the range of electron energies for which the analytic function is applicable are: A = 0.341×10^{-20} keVm^2, B = 0.424 keV and C = 4.00×10^{-20} keVm^2. Data that are used to obtain the fitting parameters are: Nickel et al. [33] in 10-300 eV range; Zecca et al. [18] in 100-3000 eV range.

The criteria adopted for the choice of data to evaluate the parameters are: 1) A wide coverage of energy range should be available to ensure a better consistency. 2) Data from the same group who measured all the noble gases to minimize systematic errors. Number of experimental

points considered were 41 in the energy range 14-3000 eV. In the discussion of total cross sections in rare gases we distinguish two ranges: A, 20 to 1000 eV and B, 0 to 20 eV.

Since the equation developed by Brusa et al. [17] is entirely empirical, the formula developed by Garcia et al. will be discussed briefly. The total cross section is the sum of the total elastic (Q_{el}) and inelastic collision cross sections (Q_{inel}). The Born-Bethe approximation for these cross sections are,

$$Q_{el} = 4\pi a_0^2 \left[A_{el}\left(\frac{R}{\epsilon}\right) + B_{el}\left(\frac{R}{\epsilon}\right)^2 + C_{el}\left(\frac{R}{\epsilon}\right)^3 + \cdots \right] \quad (8)$$

$$Q_{inel} = 4\pi a_0^2 \left[M_{inel}^2 \left(\frac{R}{\epsilon}\right) \ln\left(4C_{inel}\frac{\epsilon}{R}\right) + \cdots \right] \quad (9)$$

In equations (8) and (9) the symbols have the following meaning: ϵ is the electron energy in eV, R the Rydberg constant (= 13.60 eV), a_0 the Bohr radius, A_{el}, B_{el} and C_{el} are parameters defined as [21]

$$A_{el} = 8\int_0^\infty |Z - F(K)|^2 K^{-3} dK \quad (10)$$

$$B_{el} = -Z^2 \quad (11)$$

$$C_{el} = 0 \quad (12)$$

where Z is the nuclear charge, K is the momentum transfer and $F(K)$ is the atomic form factor. Further M^2_{inel} and C_{inel} are defined by Inokuti et al. [22] as a function of the dipole-oscillator strength density per unit of excitation energy in the atom. By adding equations (8) and (9) one gets the total cross section in the Born-Bethe approximation as

$$Q_T = a_0^2 \left[A_{tot}\left(\frac{R}{\epsilon}\right) + B_{tot}\left(\frac{R}{\epsilon}\right)\ln\left(\frac{\epsilon}{R}\right) + C_{tot}\left(\frac{R}{\epsilon}\right)^2 \right] \quad (13)$$

The values of the various symbols in argon are $A_{el} = 231$, $B = -324$, $C_{el} = 0$, $M_{inel} = 2.255$, $C_{inel} = 0.8114$, $A_{tot} = 800.9$, $B_{tot} = 63.90$ and $C_{tot} = -1018$, all in atomic units.

Garcia et al. [26] have retained the inelastic cross section contribution to the total cross section, equation (9) and obtained the expression for the elastic collision contribution as

$$Q_{el} = \frac{4\pi}{k^2} \sum_{l=0}^{l_{max}} (2l+1) \sin^2 \delta_l \quad (14)$$

where k is the momentum of the incident electron ($k^2 = \epsilon/R$ in atomic units) and δ_l is the phase shift of the l^{th} partial wave. By computing the wave shift Garcia et al. [26] have theoretically calculated the total cross sections in Ar in the energy range 0.5 k $\le \epsilon \le$ 10 k eV. A further semi-empirical equation is also given by Garcia et. al. [26]

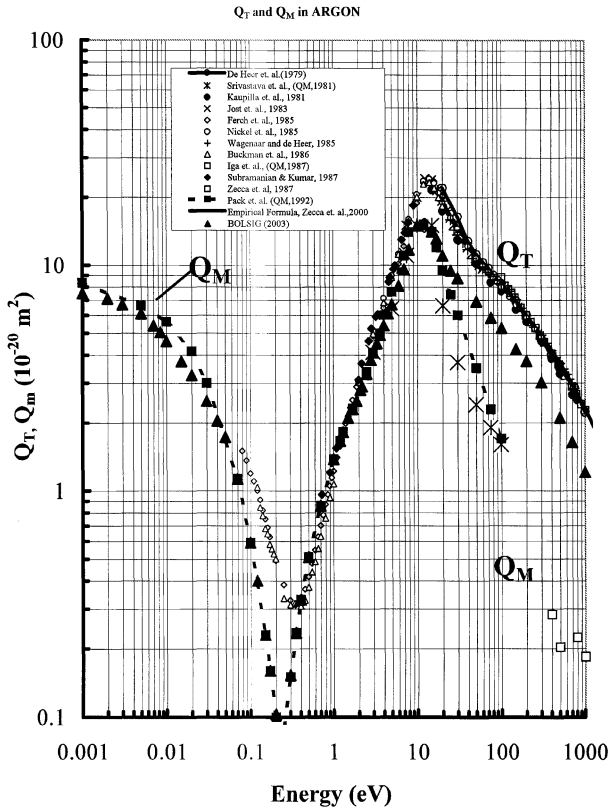

Figure 1. Total and momentum transfer cross sections in argon. Total cross sections: —●—, de Heer et al., [55]; ●, Kaupilla et al. [56]; ×, Jost et al. [34]; ○, Nickel et al. [33]; ◇, Ferch et al., [37]; +, Wagenaar and de Heer [34]; △, Buckman et al. [38]; – –, Garcia et al. [26]; □, Zecca et al. [30]; ◆, Subramanian and Kumar [59]; ——, empirical formula of Brusa et al. [17] with the correction shown in Zecca et. al. [18]. Momentum transfer cross sections: ×, Srivastava et al. [60], ○, Iga et al. [47] ■, Pack et al. [61]. Broken line is drawn as a guide. Compiled by the author.

as

$$Q_T = \left[1 - \alpha \exp\left(-\frac{1}{\beta}\frac{\epsilon}{R}\right)\right] Q_T^{BB} \quad (15)$$

where $\alpha = 0.475$, $\beta = 425$ (Ryd).

Equation (15) is attractive for application because it has theoretical basis, but it suffers from the disadvantage that the Born-Bethe approximation is generally more suitable for electron energies greater than 500 eV. We have therefore used the empirical equation of Brusa et al. [17] as reference for comparing available cross section data.

Figure 1 shows the total and momentum transfer cross sections of thirteen investigations covering the period 1979–2000. The figure also shows the total cross sections in argon, calculated according to the function (7) and using the fitting parameters given. The curve is almost obscured by the density of experimental points lying on it, indicating the degree of accuracy that the function has achieved. It is appropriate here to note that the scattering cross sections are much larger in heavier rare gases than in helium or neon particularly at low electron energies.

 1070-9878/04/$20.00 © 2004 IEEE

For example at 10 eV electron impact energy the total cross section in helium is 4.3×10^{-20} m^2 which is approximately 20% of the cross section in argon at the same impact energy. Figure 2 shows the percentage differences with the semiempirical formula of Brusa et al. [17], as corrected by Zecca et al. [18]. These two figures are briefly commented upon below.

a) Kauppila et al. [56]: The total cross sections are measured by these authors employing the beam transmission method over a wide range of electron energy of 15-800 eV. The influence of the projectile (positron and electron) on the cross sections in the same target gas is also investigated. A confining longitudinal magnetic field is employed to guide the electron beam in the electron geometry. Discrimination of small angle forward scattering of electrons is accomplished by a retarding potential technique. The special feature of these measurements are that the range of energy covered is $15-800$ eV for helium, neon and argon atoms. The semiempirical values of Brusa et al. [17] are generally lower, in the range of $5-10\%$, reaching a maximum of 12.6% at 30 eV.

b) Nogueira et al. [57]: These authors used the transmission method for measuring the total cross sections in argon in the energy range of 500–3000 eV. A correction factor is introduced that increased the quoted values of the cross section by about 3% at 500 eV and about 6% at 1000 eV. Their results are not included in Figures (1) and (2).

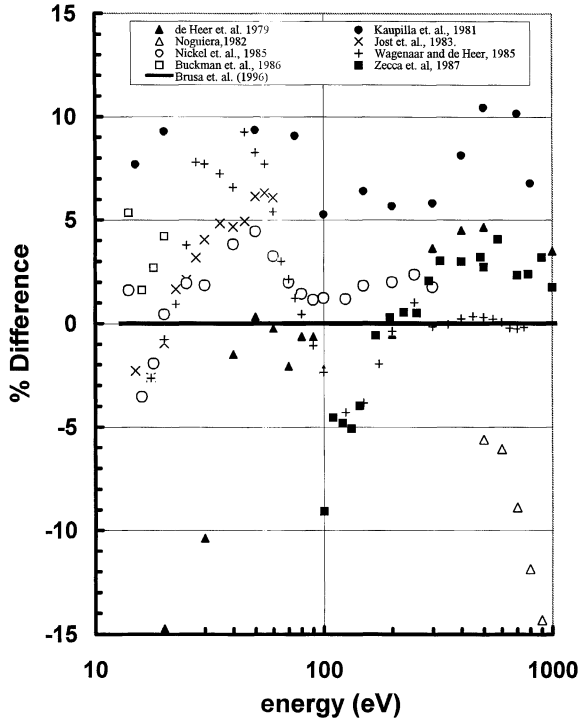

Figure 2. Percentage differences of total cross sections in argon with equation (6) as reference. ▲, de Heer et al., [55]; ●, Kaupilla et al. [56]; △, Noguiera et al. [59]; ×, Jost et al. [34]; ○, Nickel et al. [33]; ◇, Ferch et al., [37]; +, Wagenaar and de Heer [34]; △, Buckman et al. [38]; ×, Garcia et al. [26]; □, Zecca et al. [30]; ——, empirical formula of Brusa et al. [17] with the correction shown in [18], Compiled by the author.

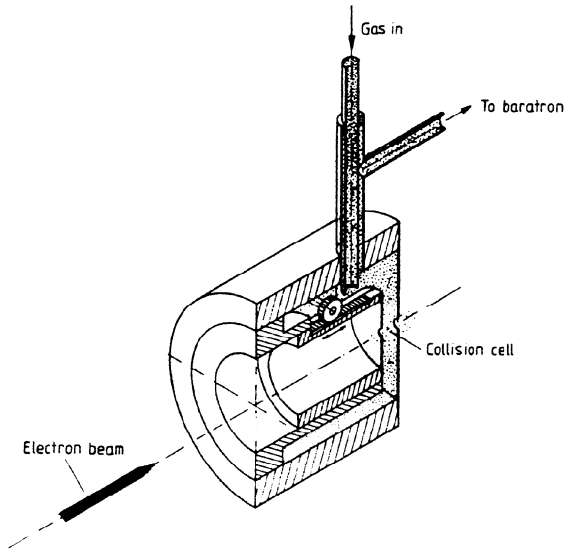

Figure 3. Experimental collision cell of Waagenar and de Heer [34] with variable collision length in the range of 0.2–10 mm for measurement of total collision cross section in argon. (Figure reproduced from Waagenar and de Heer, [34].

c) Jost et al. [32]: Tabulated values of total collision cross sections in the range of 7.5-60 eV are given in Wagenaar and de Heer [34], see below.

d)Wagenaar and de Heer [34, 58]: To remove the source of error in the Ramsauer method (section 3) Wagenaar and de Heer [58] used the linear transmission technique, avoiding the complications of the magnetic fields. Absence of the magnetic field is advantageous in the sense that the scattering geometry can be calculated without ambiguity, so the angular resolution may be defined exactly. The electrons scattered through a small angle, however, enters the detector and they are registered as unscattered electrons. Reducing the angular aperture of the detector to exclude such scattered electrons improves accuracy. The earlier investigations of [58] yielded results that were not in agreement with the subsequent results of Kauppila et al. [56] who used a linear transmission method with longitudinal magnetic fields.

To resolve the discrepancies, these authors devised an improved collision cell in which the length could be varied (Figure 3) from 0.2–10 mm. The smaller length allowed higher gas number densities, typically of the order of 1 Pa, thereby reducing calibration errors. Further, the cut off angle for screening against electrons scattered over small angles is reduced to 0.3–0.5°, from an average value of 6° that existed in the setup of Kauppila et al. [56]. The results of ref. [34] in argon are an improvement of their own earlier result by $3-7\%$ and the former are shown in Figure 1. Improved agreement with the results of Kauppila et al. [56] is also achieved.

e) Ferch et al. [37]: Time of flight method is used with a magnetic field and time to pulse height analyzer in the energy range of $0.08-20$ eV. Their results are not included in Figure 2 due to the fact that the energy range is below that discussed in this section. Their results will be commented upon with reference to Figure 3.

e) Nickel et al. [33]: The experimental set up of Nickel et al. [33], adopts the linear transmission technique and their investigations cover the incident energy range of 4–300 eV. Good agreement is obtained between their cross sections and the results of Kauppila et al. [56], Wagenaar and de Heer [34] and Jost et al. [32]. There is a maximum difference of about 13% between these measurements in the low energy range of 10–20 eV; Nickel et al. [33] obtain a maximum cross section of 24.16×10^{-20} m^2 at 14 eV. The stated accuracy, after considering all systematic errors, is $\pm2\%$.

f) Garcia, et. al. [26]: The range covered is 700–6000 eV by the transmission beam technique employing the attenuation principle. In the high energy range, electrons inelastically scattered in the forward direction can make not insignificant contributions. In order to avoid this effect an electrostatic energy analyzer is used to improve accuracy. Investigations of total scattering cross sections in the high energy range, $500-1000$ eV are limited in number (see Figure 1).

The result of Wagenaar et al. [58] in a single overlapping energy of 700 eV agrees with these measurements of Garcia et al. while the values of Kauppila et al. [56] are about 13% lower. The cross sections measured by Noguiera et. al. [57] are possibly subject to the contributions made by small angle inelastic collisions. They have applied correction factors calculated theoretically and the correction appears to be overestimated, as proved in section 9.

g) Buckman and Lohmann [38]: These authors measured the total scattering cross sections for low energy electrons in the range 0.1–20 eV using the time of flight spectrometer. The method employed is the same as Ferch et al. [37] except that a magnetic field is not employed for steering the electron beam. Their results are not included in Figure 2 due to the fact that the energy range is below that discussed in this section. Their results will be commented upon with reference to Figure 3.

h) Subramanian and Kumar [59]: A novel technique based on the photo ionization effect is employed in this investigation. The principle of the method is to use vacuum ultraviolet radiation to ionize a source gas; two electrons having different energies are obtained and by varying the source gas and VUV radiation wavelength seventeen electrons having different energies are obtained. The disadvantages of the method are that the impact energy of the electrons is not independently variable and accurate comparison with other investigations requires interpolation of data.

i) Zecca et al. [30]: The principle of the method adopted is that due to Ramsauer, with five apertures installed in the magnetic sector to obtain beam forming and selection. A modified scattering chamber is the notable feature of their setup. In the Ramsauer experimental method, simultaneous measurement of the collector current (I_c) and the scattering chamber current (I_s) is measured at any given gas number density and the ratio $I_c/(I_c+I_s)$ gives the attenuation factor. In the ideal case, the scattering current should be zero at high vacuum, as there will not be any scattering.

Zecca et al. made a comparison of their results with the semi-empirical data of de Heer et al. [55] as reference, and with the results of Nickel et al. [33], Wagenaar and de Heer [58], Kauppila et al. [56], Garcia et al. [26], in the range of 100–3000 eV. The measurements of Wagenaar and de Heer [43] are generally higher, those of Kauppila et. al. [56] generally lower, and the best agreement is obtained with the values of Nickel et al. [33]. A further observation is that the above investigations showed good agreement at 100 eV. No special conclusion is drawn except that all of the measurements quoted, except that of Garcia et al. [26] fall within a band of $\pm5\%$.

The semi-empirical values of de Heer et al. [55] lie in the range of -15% at 20 eV, gradually increasing to about 3% at 1000 eV. The results of Kauppila et al. [56] fall in the upper range of $+5-13\%$ the largest discrepancy occurring at 30 eV. The values of Jost et. al. [32], Wagenaar and de Heer [58], Nickel et al. [33], and Zecca et al. [30], lie in a band of $\pm5\%$. Of course we should recall that the constants of semi-empirical of equation (7) were derived using the data of the latter two publications, in the $20-300$ eV range and $100-3000$ eV range, respectively.

j) Furst et al. [40]: The time of flight method with a rotatable detector in the energy range of 3–20 eV is used. Their results are not included in Figure 2 due to the fact that the energy range is below that discussed in this section. Their results will be commented upon with reference to Figure 3.

We now consider the momentum transfer cross sections in a general way. Srivastava et al. [60] measured the differential cross sections for elastic collisions and obtained both the momentum transfer and elastic collision cross sections by the application of equations (1) and (3) . They employed an apparatus that consists of an electron scattering spectrometer, gas flow system, and a multichannel analyzer for detecting and storing the scattered electron signal. The experimental gas effused through a capillary producing a well-defined beam of atoms, at 90° to the electron beam. Differential cross sections, covering the electron energy range of $3-100$ eV, and an angular range of $-35°-130°$ with respect to the direction of the incident electron beam, were measured. The normalization is with respect to helium. Iga et al. [47] also measured the

differential cross sections and thereby calculating the elastic and momentum transfer cross sections.

The momentum transfer cross sections cannot be measured below a certain minimum energy due to experimental limitations. To extend the range of the electron energies towards the lower limit, Pack et al. [61] employed swarm experimental results to derive the ratio of the longitudinal diffusion coefficient (D_L) to mobility (μ) in the electron energy range of 0 − 100 eV. The principle of this method essentially consists of solving the Boltzmann equation and calculating the swarm coefficients. A comparison with experimental results is then used to apply corrections to the initial cross sections, by a backward prolongation technique, first used by Engelhardt and Phelps [62]. For energies greater than 10 eV the momentum transfer cross section begins to get smaller than the total cross section; the differences increase with increasing energy.

The momentum transfer cross sections in the higher energy range of 300−1000 eV have been obtained by Iga et al. [47] in a crossed beam geometry with a small magnetic field (1.5μT). Elastic differential cross sections are measured and by integration, the integrated elastic and momentum transfer cross sections are derived, as usual. The values lie smoothly on the curve connecting the points of Pack et al. [61] (see the broken line in Figure 2). There is paucity of data in the 100-300 eV range of electron energies.

5 TOTAL CROSS SECTIONS ($0 < \epsilon \leq 15$ eV)

Total scattering cross sections in this range of electron energy have been of particular interest from the earliest studies of Ramsauer and Townsend. The Ramsauer-Townsend minimum in rare gases occurs in this range of impact energies and the phenomenon of very low cross sections in the 0-3 eV range is of interest from the theoretical aspect of application of quantum mechanics to the argon atom.

The experimental technique of Golden and Bandel [27] using the Ramsauer beam technique has already been mentioned. Milloy et al. [61] calculated the momentum transfer cross sections in argon using the drift velocity and D_T/μ up to 4 eV energy. Ferch et al. [37] used the time of flight spectroscopy in the electron impact energy range of 0.08−20 eV range.

These results are summarized in Table 2 where the apertaining cross section is also shown. While the cross section minimum is observed to occur at approximately 0.25−0.285 eV except by Ferch et al. [37], the magnitude of the minimum cross section differs by a factor of about 3.5, the highest being observed by Ferch et. al. [37] and Buckman and Lohmann [38]. The lowest cross section is due to Pack et al. [61]. It is difficult to reconcile such a large difference, even allowing for the fact that Ferch et al. [37] obtained total cross section whereas Pack et al. [61] derived momentum transfer cross sections. The dominance of the p-wave contribution to the total cross section in the Ramsauer-Townsend region increases the forward scattering. It is possible that the results of Golden and Bandel [27] are low in this energy region because of poor discrimination against forward scattering of electrons. In the time of flight method adopted by Buckman and Lohmann [38] the energy resolution is estimated to be 20 meV where as the Ramsauer-Townsend minimum has a width, in excess of 150 meV. However as the energy increases towards 1 eV the discrepancy between the results of Ferch et al. [37] and those of Buckman and Lohmann [38] increases reaching a maximum of 12%. The reasons for this discrepancy are not clearly understood as noted by Buckman and Lohmann, [38][1].

Table 2. Ramsauer-Townsend minimum cross section in argon.

Authors	Energy (eV)	Cross section ($\times 10^{-20}$m^2)	Type
Golden and Bandel [27]	0.28	0.15	Q_T
Ferch et al. [37]	0.34	0.31	Q_T
Buckman and Lohmann [38]	0.3	0.31	Q_T
Milloy et al. [62]	0.25	0.095	Q_M
Pack et al. [60]	0.25	0.091	Q_M

The total cross section extrapolated to zero energy gives a cross section, $Q_T(0)$ usually expressed by the scattering length, according to $Q_T(0) = 4\ \pi A^2$ where A is the scattering length. At zero energy the total cross section contains only the s-wave scattering and equals the momentum transfer cross section determined by swarm experiments. The scattering length determined by Pack et al. [60] is 8.92 $\times 10^{-11}$ m. Other values lie between (7.895-8.625) $\times 10^{-11}$ as quoted by Zecca et. al. [10].

6 ELASTIC TOTAL AND DIFFERENTIAL CROSS SECTIONS

The procedure followed for presenting the total cross sections is also adopted for presenting the elastic collision cross sections also. The equation of Brusa et al. [17] for elastic collision cross sections for all the rare gases except helium, in the energy range 10−10,000 eV is

$$Q_{el} = \frac{1}{A(B+E)} + \frac{1}{C(D+E)} + \frac{2}{E}\sqrt{\frac{BD}{AC}}\ \frac{1}{|B-D|}\left|\ln\frac{\frac{E}{D}-1}{\frac{E}{B}+1}\right| \quad (16)$$

[1] *A more detailed discussion on momentum transfer cross sections is included in the second paper dealing with the cross sections in the remaining gases.*

Table 3. Fitting parameters for elastic collision cross sections in rare gases (Brusa, et al. [17]).

Gas	No. of points	Energy range (eV)	A (keV^{-1} 10^{-20} m^2)	B ($keV-1$)	C (keV^{-1} $10^{-20}m^2$	D (keV)
Ar	52	10-10000	0.632	0.593	3.65	0
Kr	52	10-10000	4.115	0.0017	0.388	1.35
Ne	52	10-10000	7.7076	0.0381	3.64	1.11
Xe	48	80-10000	1.210	0.203	0.121	13.60

where ϵ is the collision energy and A, B, C and D are the fitting parameters. The values of these coefficients are shown in Table 3. The elastic collision cross section measurements usually have an uncertainty of 20-30%, arising due to the fact that the measured differential cross sections are integrated over the scattering angle. The measurements are not carried out over the entire range of angles, 0–180°, and extrapolation is required at either end of the range. This extrapolation can introduce large errors. Further, for the determination of absolute differential cross sections, normalization is required using other known experimental or theoretical cross sections.

The elastic collision cross sections used for finding the fitting parameters were obtained by Brusa et al. [17] in an indirect way; the inelastic collision cross sections were subtracted from the total cross sections. This procedure yielded cross sections that were not dependent on direct measurements and the parameters evaluated are not biased towards individual set of data.

Figure 4 shows the selected elastic collision cross sections published by several groups, along with the calculated values. For electron energies greater than 20 eV the total cross section given by Zecca et al. [18] is also given again to convey the contribution of inelastic collisions to the total cross section. De Heer et al. [55] evaluated a set of cross sections in argon and the elastic collision cross section is obtained by integrating the differential cross sections of several publications published till 1979, using equation (1) where Q_{diff} is the differential elastic cross section. The theoretical calculations of Nahar and Wadhera [63] in the energy range 3–300 eV are also shown. There is extremely good agreement between their values and the experimental results of Srivastava et al. [60] over the entire range of electron energy. The measurements of Furst et al. [40] 3–20 eV, again with reasonable agreement. The higher energy (400–1000 eV) range is covered by Iga et al. [47] whose values lie smoothly on the semiempirical curve.

Figure 5 shows the relative differences in elastic collision cross section with respect to the semiempirical equation of Zecca et al. [18] in the energy range 10–1000 eV. The percentage differences with respect to the analytical function are smaller than that one obtains by choosing one of the measured cross sections for reference. For example, at 30 eV energy, Srivastava et al. [60] measured a cross section of 9.2×10^{-20} m^2, compared with the semiempirical value of 13.94×10^{-20} m^2 due to de Heer et al. [55] at the same energy; a difference of about 50%.

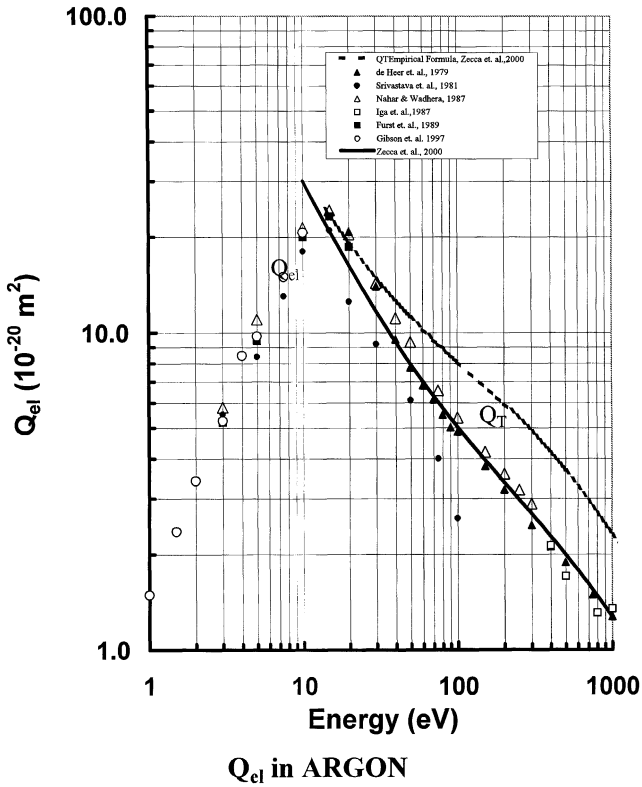

Figure 4. Integral elastic collision cross sections in argon. Full line is the semiempirical formula of Zecca et al. [18]; ▲, semiempirical data of de Heer et al. [55]; ●, Srivastava et al. [60], □, Iga et al. [47]; △ Nahar and Wadhera [63]; ■, Furst et al. [40], ○, Gibson et al. [49]. Total cross section according to Zecca et al. [18], broken curve, is included to show the contribution of inelastic collision cross sections.

Early measurements of differential cross sections are due to Webb [64] in both argon and krypton. Differential cross section data available up to 1977 have been reviewed by Bransden and McDowell [6]. Since then accurate measurements are published by: Srivastava et al. ([60], 3–100 eV, angular range 20–135°, Wagenaar et al, ([35], 20–200 eV, angular range 0–10°, Weyherter ([65], 0.05–2 eV), Zubek et al. ([66], 10 eV, 30–180°, Cvejanović and Crowe ([67], 20.4–110 eV, angular range 40–120°). The experimental set up of Wagenaar et el. [35] has the special feature of low angles at energy less than 100 eV. The experiments of Weyherter [65] and Gibson et al. [49] have the special feature of extending the lower range of elec-

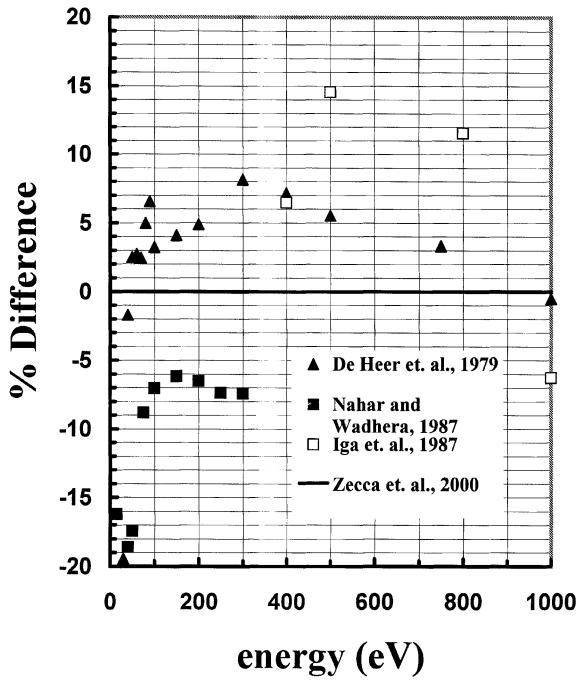

Figure 5. Percentage differences in integrated elastic cross section in argon obtained using the analytical function of Zecca et al. [18] as reference. ▲, De Heer et al. [55]; ■, Nahar and Wadhera [63], □, Iga et al., [47]. Data calculated by the present author.

tron energy, of Zubek et al. [66] to higher angles up to 180°, of Cvejanović and Crowe [67] to continuously variable electron energy.

The differential scattering cross section is a function of both the angle of scattering and the electron energy. The direct determination of absolute cross sections is exceptionally difficult and the usual method adopted to achieve the goal is to measure the relative differential cross sections and then convert them to an absolute scale by normalization to cross sections of targets for which the absolute cross sections are reliably known (Furst et. al., [40]). Helium and neon targets are used for the purpose of normalization of elastic collision cross sections.

The normalization is accomplished by two different techniques: at sufficiently low energies where only the elastic collisions occur in rare gases, phase shifts of some of the lowest order partial waves may be obtained by fitting the angular distribution measurements. These extracted phase shifts, together with higher order phase shifts obtained by the Born approximation are used to place the differential cross sections on an absolute scale. This method, known as the phase shift method (Srivastava et al., [60]) has been successful in helium, making that gas as a preferred choice for normalization.

The second method is the relative flow technique. Briefly the cross section in the target gas is measured and under identical conditions, the target gas is replaced by helium and measurements carried out at the same angles. The ratios of measured cross sections are related to the flow rates and the absolute cross section is determined. The relative flow normalization technique has also been employed in argon (Srivastava et. al., [60]), though the agreement between the two methods (relative flow and phase shift) has been poor.

Figure 6 shows the angular variation of the cross sections at selected energies due to Srivastava et al. [64], Gibson et al. [49] and Cvejanović and Crowe [67]. Srivastava et al. [64] normalized their measurements to helium, Gibson et al. [49] applied the phase shift analysis and Cvejanović and Crowe [67] normalized their relative cross sections to the absolute cross sections of Srivastava et al. [60]. The agreement between the measurements is good over the overlapping regions of energy.

The angular variation of the differential cross section depends on the electron energy. Williams and Willis [68] have measured the absolute differential elastic collision cross sections for incident electron energies from 20 to 400 eV, over the angular range of 20° to 150°, with an angular resolution of 2° and an energy resolution of 95 meV. Two minima are observed in the energy range 20−100 eV. At 150 eV the first minimum flattens to a plateau and there is one minimum occuring at $\sim 120°$. Williams and Willis [68] suggest that at these angles and below 100 eV, the larger partial waves ($l > 3$) contribute significantly to the cross section.

The energy range is extended to lower values, $0.5 \leq \epsilon \leq 20$ eV, by Williams [69] who has calculated the phase shifts for $l = 0$ to 3. The magnitude of the phase shifts as a function of energy for elastic scattering is the largest due to s and d waves, the contributions from the p and f waves having intermediate values. For example at 10 eV electron incident energy the magnitude of the contributions are 1: 0.48: 0.85: 0.08 for increasing values of l from 0 to 3 respectively. The same ratios at the lowest energy studied by Williams [69], 0.58 eV, are 1: 0.10: 0.36: 0.04. The theoretical calculations of McEachran and Stauffer [70] demonstrate that the contributions of s- and p- waves decrease, and the contribution of d-wave increases to the scattering cross section as the impact energy increases from 3 to 50 eV. The dominance of s-wave contribution, particularly at low energies, < about 2 eV, tends to make the angular dependence of the differential cross section flatter. The result of Weyherter [65] at the very low energy of 0.05 eV supports this reasoning. A qualitative comparison may be made with helium in which gas the s-wave phase shift is dominant at all energies, though there is a negligibly small contribution from the p-wave phase shifts [69]. The phase shift dependence of the differential cross section in helium at 1.5 eV energy is also relatively flat, as also in other rare gases (see Figure 6 of [10]).

Furst et al. [40] have measured the differential cross sections in the electron energy range of $3-20$ eV and angular range of $20°-130°$. Relative values are converted to

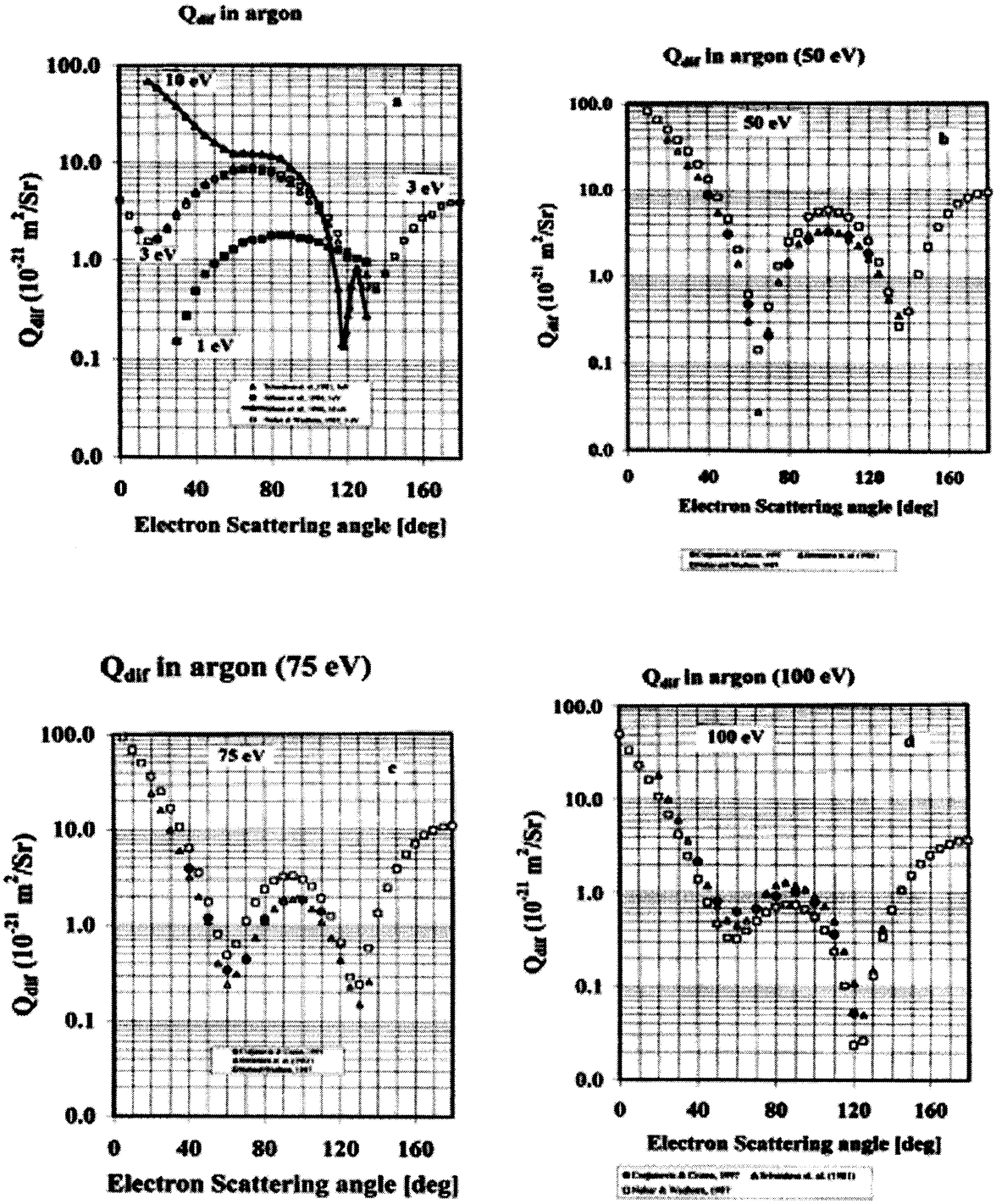

Figure 6. Differential scattering cross sections in argon as a function of scattering angle at various electron impact energies. Both experimental and theoretical results are shown. Due to experimental limitations experimental results do not cover the entire range of the scattering angle. (a) ■, Gibson et al., [49], 1 eV; △, Srivastava et al., [60], 3 eV; □, Nahar and Wadhera, [63], 3 eV; −−△−−Gibson et al., [49], 10 eV. (b) 50 eV, ●, Cvejanović and Crowe, [67]; □, Srivastava et al., [60]; □, Nahar and Wadhera, [63]. (c) 75 eV (d) 100 eV. Symbols for (c) and (d) same as for (b). Compiled by the author.

absolute scale by both the phase shift analysis and relative flow method. The two sets of absolute differential cross sections obtained are in excellent agreement with each other; an improvement over the results of Srivastava et al. [64]. The angular dependence of the differential cross sections of Furst et al. [40] may be combined smoothly with the theoretical values of McEachran and Stauffer [70] for lower angles ($< 20°$) as there is very good agreement between the two sets of results. Two minima are clearly seen even at the low energy of 3 eV.

The explanation for observing two minima, particularly at energies 3 − 100 eV is substantially due to Furst et. al. [40]. For a heavy rare gas atom such as argon, the validity of the phase shift analysis at any energy is not generally successful. Due to the higher polarizability of the atom, higher order partial waves make a greater contribution to the scattering cross section, at any energy. The effect of the higher order contribution is to cause a more pronounced forward peak in the differential scattering cross sections. The relatively large *d*-wave contribution causes distinct minima in the differential cross sections at low energies. As the energy increases the *d*-wave contribution dominates, resulting in a shift of the minima with electron energy (Furst et. al., [40]). At 75 and 100 eV two minima can be seen (Figure 6), and theoretical calculations by Nahar and Wadhera [63] also confirms the existence of two minima at electron energies $3 \leq \epsilon \leq$. 100 eV. It is noted that the experiments of Weyherter [65] are uniquely at low energies (0.05-2 eV) while other investigations, both theoretical and experimental are at higher energies. The author is not aware of any publication that reports conflicting features of the ϵ-Q_{diff} curve at the same electron energy with regard to the existence or absence of two minima, lending support to accept the above reasoning.

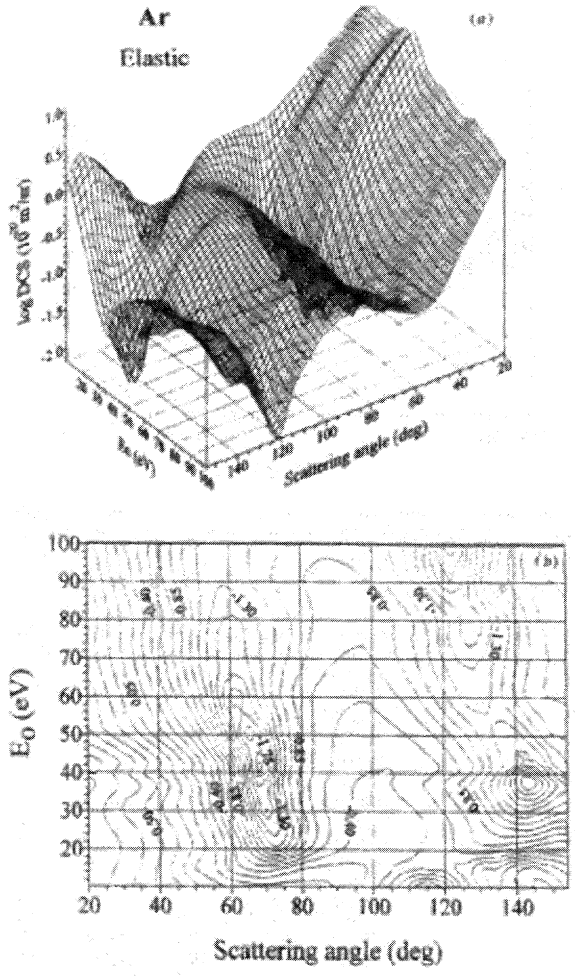

Figure 7. Differential cross sections (DCS) for elastic electron scattering by argon in the angular range 20°−150° at incident energies from 10 to 100 eV: (a) three dimensional representation of the DCS (E_0, θ) surface shown on a logarithmic scale; (b) projection of the DCS (E_0,θ) surface on the horizontal plane. Numbers correspond to the logarithm of the DCS values in units of 10^{-20} m^2sr^{-1}. (Figure reproduced from Panajović et al., [71]). Figure (b) touched up for better reproducibility.

A three dimensional plot of the differential cross sections as a function of the scattering angle at various energies shows two global minima, one at low angle and the other at a higher angle as shown in Figure 7 [71]. Theoretical verification of these results are provided by Sienkiewicz et al. [72], and the observed critical minima (39.3 eV, 68°) and (39.5 eV, 141°) agree with the measurements of Panajotović et al. [71]. The critical minimum points serve as a check for the accuracy of measurements and calculations in argon.

7 TOTAL EXCITATION CROSS SECTIONS

Excitation of atoms and molecules by electron impact results in radiation output or generation of metastable states which return to ground state by indirect means, such as being de-excited to a different allowed level by a collision. The total excitation cross section is required for the purposes of discharge simulation, finding the solution of Boltzmann equation, etc. and detailed discussion of excitation to every allowed level will not fall into the domain of our requirement; in argon alone there are over 75 lines. A review of electron impact excitation cross sections in atoms covering 1968 is given by Moiseiwitsch and Smith [73]. Electron excitation of metastable atoms has been reviewed by Fabrikant, et al. [74] and electron impact optical excitation functions are reviewed by Heddle and Gallagher [75].

Argon has 18 electrons with the outer electron shell associated with the principle quantum number $n = 3$ in the $3s^2\ p^6$ configuration. Within 14.3 eV of the ground state, there are thirty electronic states. Of the first four levels, level 1 ($4s\ [3/2]_2$, onset energy 11.548 eV) and level 3 ($4s'[1/2]_0$, onset energy 11.675 eV) are metastables; their life times are 55.9 and 44.9*s*, respectively (Filipović et al. [76]). Level 2 ($4s\ [3/2]_1$, onset energy 11.631 eV) and level 4 ($4s'[1/2]_1$, onset energy 11.723 eV) radiate to ground level with emission wave length of 106.6 nm and 104.8 nm, respectively. A partial energy level diagram of argon is shown in Figure 7 and twenty five levels with appearance potentials are shown in Table 4.

The cross sections for the first 23 states due to Chutjian and Cartwright [11] in the electron energy range of 16 − 100 eV, covering both the forward and backward hemispheres, have been recognized as benchmark measurements. The adopted values of electron energies are 16, 20, 30, 50 and 100 eV; the energy loss of the scattered electrons are measured. The scattering angle ranges from 5°−138° and differential excitation cross sections are extrapolated to 0° and 180° to yield integral cross sections.

Table 4. Excitation levels in argon. Racah notations are taken from Chutjian and Cartwright [11]. The threshold energy and Paschen notations are due to Hayashi [77].

Level number	Threshold energy (eV)	Racah notation	Paschen notation
1	11.55	$4s[3/2]_2^0\ ^3P_2$	$1s_5$
2	11.62	$4s[3/2]_1^0\ ^3P_1$	$1s_4$
3	11.72	$4s'[1/2]_0^0\ ^3P_0$	$1s_3$
4	11.83	$4s'[1/2]_1^0\ ^1P_1$	$1s_2$
5	12.91	$4p[1/2]_1$	$2p_{10}$
6	13.08	$4p[5/2]_3$	$2p_9$
7	13.09	$4p[5/2]_2$	$2p_8$
8	13.15	$4p[3/2]_1$	$2p_7$
9	13.17	$4p[3/2]_2$	$2p_6$
10	13.27	$4p[1/2]_0$, $4p'[3/2]_1$	$2p_5$, $2p_4$
11	13.03	$4p'[1/2]_2$	$2p_3$
12	13.33	$4p'[1/2]_1$	$2p_2$
13	13.47	$4p'[1/2]_0$	$2p_1$
14	13.84	$3_d[1/2]_0^0$, $3d[1/2]_1^0$	$3d_6$, $3d_5$
15	13.90	$3_d[3/2]_2^0$	$3d_3$
16	13.98	$3d[7/2]_4^0$	$3d_{4'}$
17	14.01	$3d[7/2]_3^0$	$3d_6$
18	14.06	$3d[5/2]_2^0$, $5s[3/2]_2^0$	$3d_{1''}$, $2s_5$
19	14.09	$3d[5/2]_3^0$, $5s[3/2]_1^0$	$3d_{1'}$, $2s_4$
20	14.15	$3d'[5/2]_2^0$	$3d_2$
21	14.21	$3d'[5/2]_2^0$	$3s_{1''''}$
22	14.23	$3d'[3/2]_2^0$, $3d'[5/2]_3^0$, $5s'[1/2]_0^0$, $5s'[1/2]_1^0$	$3s_{1''''}$, $3s_{1''}$, $2s_3$, $2s_2$
23	14.30	$3d'[3/2]_1^0$	$3s_{1'}$
24	14.71	$4d[1/2]_1$	$4d_5$
25	15.20	$6p'[1/2]_1$, $6p'[3/2]_1$, $6p'[3/2]_2$	$4p_2$, $4p_4$, $4p_3$

Hayashi [77] has provided cross sections to additional two states, twenty five in all, with the added advantage that the cross sections are presented in a range of electron energies, up to 1000 eV. Figure 9 shows these individual cross sections.

The sums of their cross sections are shown in Figure 10. The total cross section reaches a peak in the region of 30–50 eV with a cross section of 0.9×10^{-20} m^2.

Optical measurements of excitation cross sections are classified as apparent excitation cross sections and cascade excitation cross sections. An electron beam traverses the gas, exciting some atoms to level i as they fall to a lower level j, the resulting radiation is detected to measure the optical emission cross sections (Q_{ij}^{opt}). The sum of all emissions to lower states is termed the apparent excitation cross sections for the level i:

$$Q_i^{\text{app}}(\text{ex}) = \sum_{j<i} Q_{ij}^{\text{app}}(\text{ex}) \tag{17}$$

A level i may be populated both by direct electron impact excitation and by higher exciting levels cascading into it. The cascade cross section is the sum of all optical cross sections for the transition into the level from higher levels

$$Q_i^{\text{cas}}(\text{ex}) = \sum_{k>i} Q_{ki}^{\text{opt}}(\text{ex}) \tag{18}$$

The direct electron excitation cross section is obtained as the difference between the apparent cross section and the cascade contribution (Filippelli et al., [78])

$$Q_i^{\text{dir}}(\text{ex}) = Q_i^{\text{app}}(\text{ex}) - Q_i^{\text{cas}}(\text{ex}) \tag{19}$$

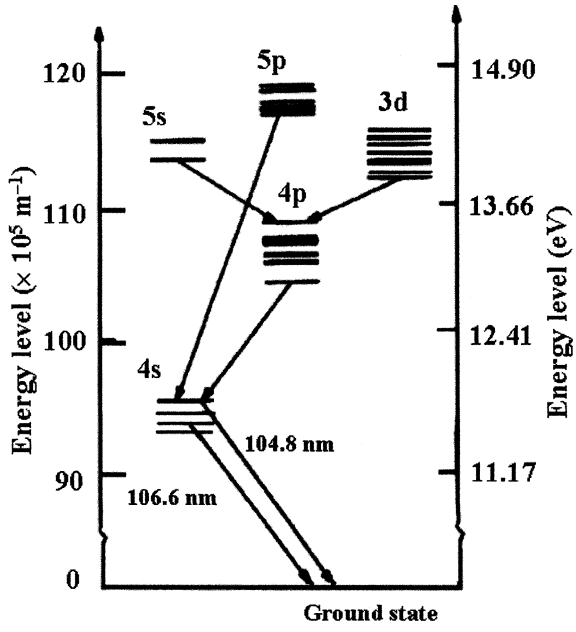

Figure 8. Partial energy diagram of argon (adopted from Tsurubuchi et al. [81].

McConkey and Donaldson [32], for example measured the apparent excitation cross sections by optical methods.

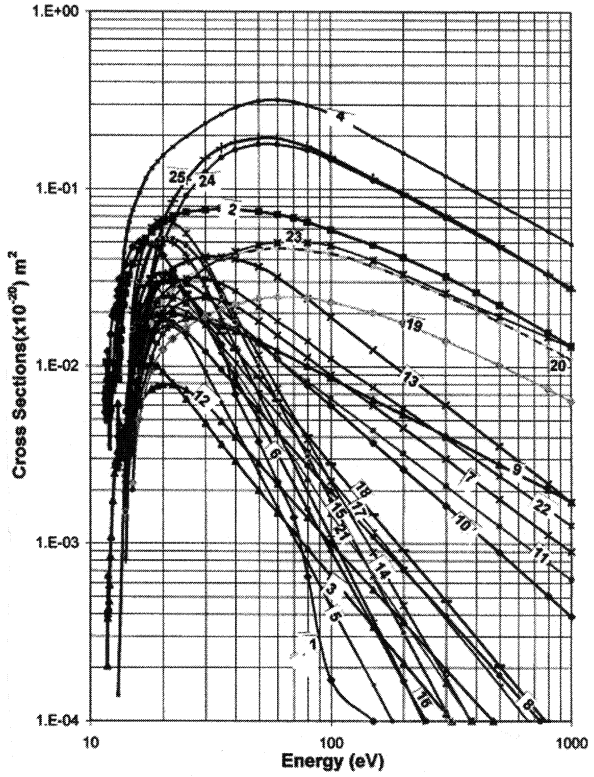

Figure 9. Excitation cross sections for 25 levels of argon (Hayashi [77]). Plotting is due to Syed Ul-Haq. See reference [20] of Phelps and Petrović [100].

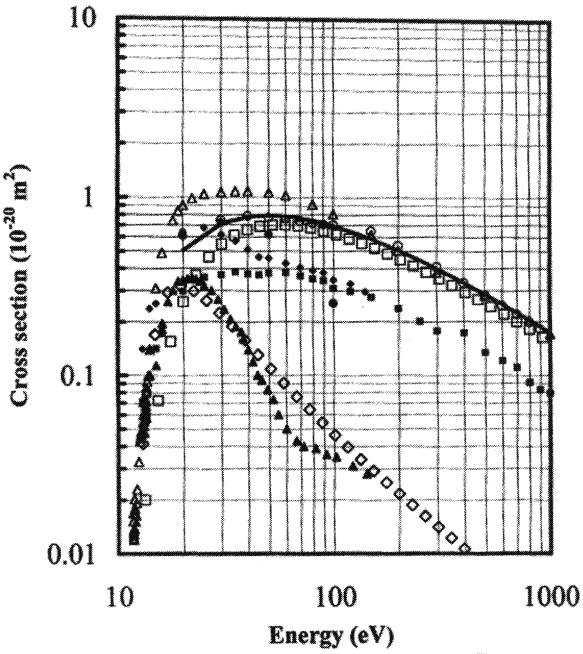

Figure 10. Excitation cross sections in argon. ▲, Mason et al. [39] -total metastable states; ●, Chutjian et al. [11] -total excitation cross sections for the first 23 levels; □, Tsurubuchi et al. [81] -sum of lower resonance cross sections; ♦, Tsurubuchi et al. + Mason et al; ○, de Heer et al. [55] -total excitation; —, Brusa et al. [17] -total excitation, ◇, Pitchford et al. [83] -total metastable; □, Pitchford et al. [83] -total resonance states. Total cross section (Hayashi [77]), compiled by the author.

Most of the cascade contribution in argon is in the infrared region (Chilton et. al., [79]) and a Fourier transform spectrometer has been used by them to determine the direct excitation cross sections.

Cross sections for some or all of the first four levels, consisting of two metastable states and two resonance levels are measured in recent years by the following: McKonkey and Donaldson [32] — > level 2 + level 4; Mason and Newell [39] — > total metastables including level 1 + level 3; Mityureva and Smirnoff [80] — > level 1 + level 3; Tsurubuchi [81] — > level 2 + level 4; Filipović et al., [76] — > level 4, Filipović et al., [82] — > level 1+ level 2+ level 3. The values of Tsurubuchi [81] for the lowest resonance states and values of Mason and Newell [39] for the total metastable levels are shown separately in Figure 10. The more recent results of Chilton et. al. [79] are not included as tabulated results are not given in the original publication. The total excitation collision cross section obtained by adding these two cross sections in the range of 13—142 eV, merging smoothly with the cross sections of Tsurubuchi [81] for energies greater than 142 eV are also shown. A comparison is shown in Table 5.

As the previous discussion reveals there are relatively few data available on the total excitation cross sections from onset to 1000 eV range. At the onset energies in the range 12–30 eV there is considerable disagreement between various results. One of the more frequently used total excitation cross sections in argon is due to de Heer et al. [55] who covered the range of 20–4000 eV. Since Tsurubuchi's results [81] shown in Figure 9 cover only two optical levels, their cross sections are obviously lower than those due to de Heer et al. [55]. Brusa et al. [17] have suggested a semiempirical expression from threshold to several keV energy

$$Q_{ex} = \frac{1}{F(G+\epsilon)} \ln \frac{\epsilon}{\epsilon_{exc}} \tag{20}$$

where ϵ is the incident electron energy, F and G, the two adjustable parameters, and ϵ_{ex} is the excitation threshold energy (Table 6). The source for finding the fitting parameter for argon is de Heer et al. [55]. The equation agrees very well with the semiempirical values of de Heer et al. [55] over the entire range, 20- eV. In this range the total excitation cross sections adopted by Pitchford and Morgan [83] for solving the Boltzmann equation also agree very well with the equation of Brusa et al. [17].

8 IONIZATION CROSS SECTIONS

The technique and results of measurements of ionization cross sections in argon by Rapp and Englander-Golden [84], stood the test of time, with a quoted uncer-

Table 5. Comparison of measured excitation cross sections in argon in units of 10^{-23} m^2.

	Level 1 ($4s[3/2]_2$)					
	Range eV	Energy (eV)				
		20	40	60	80	
Chutjian & Cartwright [11]	16–100	31.9				
Mityureva & Smirnoff [80]	Onset–60	300	145			
Schappe et al.[1]	Onset–100	40	7.6			
Filipović et al. [78]	20–80	53	18			
Hayashi [77]	Onset–200	46.4	13.2	3.75	1.41	
		Level 2 ($4s[3/2]_1$)				
	Range eV	Energy (eV)				
		20	40	50	80	
McConkey and and Donaldson, [32]	10–2000	50	83	92	86	
Chutjian and Cartwright [11]	16–100	37		57.8		
Tsurubuchi et al. [81]	Onset–1000	153	135	120	110	
Filipović et al. [78]	20–80	69	93	74	53	
Hayashi [77]	Onset–1000	65.8	76.5	74.3	65.0	
		Level 3 ($4s'[1/2]_0$)				
	Range eV	Energy (eV)				
		20	40	50	80	
Chutjian & Cartwright [11]	16–100	6.44				
Mityureva & Smirnoff [80]	Onset–60	75				
Schappe et al.[1]	Onset–100	13.5	3.4			
Filipović et al. [78]	20–80	12	6.3			
Hayashi [77]	Onset–1000	9.23	2.9	2.0	9.3	
		Level 4 ($4s'[1/2]_1$)				
	Range eV	Energy (eV)				
		16	20	30	40	50	60
McConkey et. al. [32]	10–2000		170	250	260	220	225
Chutjian and Cartwright [11]	16–100	85.3	100	144		214	
Tsurubuchi et al. [81]	Onset–1000	145	194	237	257	269	
Filipović et al. (76)	20–80	150	176	297	313	295	193
Mason & Newell [39]	12–142	195	345	251	139	80	50
Hayashi [77]	Onset–1000	94.7	15.4	23.3	28.8	31.3	31.8

Table 6. Parameters for total excitation cross sections in argon (Brusa et al., [17]).

Gas	No. points	Energy range (eV)	ϵ_{ex} (eV)	F (keV^{-1} 10^{-20} m^2)	G keV
Ar	22	20–3000	11.5	25.19	23.6×10^{-3}
He	11	20–500	19.8	77.65	0
Ne	21	30–4000	16.619	85.97	31.7×10^{-3}
Kr	22	20–4000	9.915	22.0	23.3×10^{-3}
Xe	18	80–1000	8.315	18.27	0

tainty of 7% and they may be employed as basis, to determine the differences between more recent literature. The method adopted fall into the category of beam-static-gas category, though they employed the gas flow method to determine the pressure, instead of an absolute gauge. The total ionization cross sections are measured by collecting all the ions generated. Though the concept is rather simple, accurate measurements have proved to be difficult, due to the fact that uncertainties exist in the determination of various parameters involved (Keiffer and Dunn, [85]). Rapp and Englander-Golden [84] measured the total ionization cross sections and partial ionization cross sections could not be determined by their method.

The main sources of uncertainty in the measurements of electron ionization cross sections are [86]: (1) Absolute measurement of number of electrons striking the molecules. (2) The number of ions created. (3) The interaction path length. (4) The detector efficiency for differently charged ions in case of partial ionization measurements and (5) the target gas density at a pressure which is of the order of 10 mPa. Sorokin et al. [86] suggest that the first four sources may be easily eliminated by measuring cross sections using photon flux and the measurements may be carried out at relatively higher pressure of the order of 100 Pa. The cross sections that have been determined in rare gases using photon beams are well known with an uncertainty of $1-3\%$, which is a considerable improvement over the electron impact ionization measurements.

Partial ionization cross sections are defined as cross sections describing the electron impact production of an ion of specific charge n, according to e + X-> X^n + (n +

1)e. To determine the partial cross sections a mass spectrometer is required and the earlier results of 1930's suffered from errors due to the assumption of a constant ion collection efficiency for ions of differing charges. Stephan et al. [87] improved the mass spectrometer method ensuring controlled extraction and collection of ions. Their results provided cross section data in all rare gases from the same laboratory using the mass spectrometer method. Relative cross sections were obtained and from these, absolute values were determined by normalizing to the cross section of Rapp and Englander-Golden [84] at a specific energy.

Ionization cross sections may be measured by the electron impact or photon impact; the ratio of the cross sections determined by both methods has been exploited to improve the accuracy of electron impact cross sections; this aspect will be referred to later on. As the electron energy increases, double or multiple ionization occurs and the total ionization cross sections (Q_i) may then be expressed in two different ways, depending upon the technique employed for the cross section measurements. In the first way, the partial sum of the cross section at each ionization potential is added according to

$$Q_{i,\text{count}} = Q_i^+ + Q_i^{2+} + Q_i^{3+} + \ldots \qquad (21)$$

where Q_i^+ is the cross section for singly charged ion, Q_i^{2+} is the cross section for doubly charged ion and so on. The gross ionization cross section, on the other hand, is the charge weighted sum of the partial ionization cross sections:

$$Q_{i,\text{gross}} = Q_i^+ + 2Q_i^{2+} + 3Q_i^{3+} + \ldots \qquad (22)$$

Methods that employ measurement of total ion current fall into this category.

Reviews of ionization cross sections are published by Kieffer and Dunn [85], Märk [88], and Lennon et al. [89]. Differences in the early results of Asundi and Kurepa [90] and Schram et al. [91-94] when compared with the results of Rapp and Englander-Golden [84] show that the path length and difficulties of pressure measurement are the sources of error. Contamination of mercury vapor is also a significant source of error.

Selected measured cross sections are shown in Figure 11. For the purpose of clarity of presentation the available data are presented as two sets of curves. In the first set (lower curve of Figure 10) the cross sections as determined by several authors as shown. In the second set (top curve) the cross sections are multiplied by a factor of ten. Fletcher and Cowling [95] have measured the total absolute cross sections in the range of 16-500 eV by using a pulsed electron gun. A special feature of their setup is that the ionization cross sections and ionization coefficients are measured simultaneously so that the purity of the gas remains the same in both measurements. The technique adopted is similar to that of Rapp and Englander-Golden [84]; measuring the total ion current produced by a monoenergetic electron beam of well defined energy, passing through a layer of gas, in a beam- static-gas configuration.

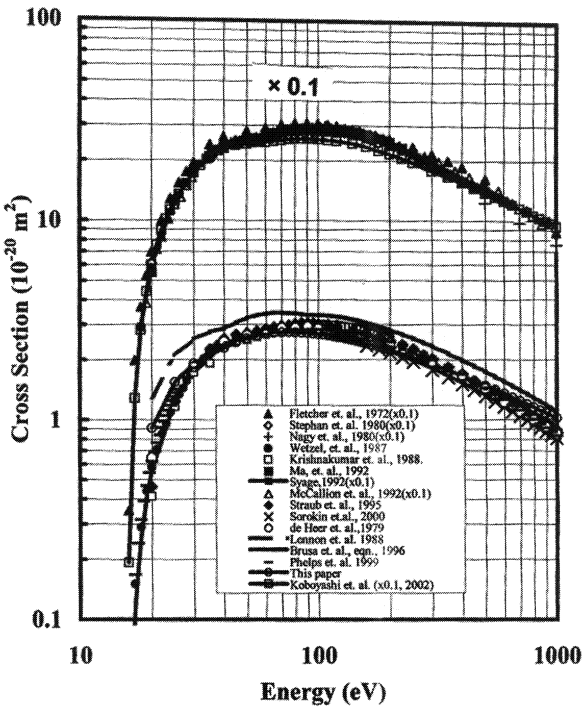

Figure 11. Absolute total ionization cross sections in argon. The data are presented by two curves for more clarity. The values shown by the top curve should be multiplied by 0.1. Experimental: ♦, Fletcher and Cowling, [102]; ◇, Nagy et al., [97]; – –, Wetzel et al., [50]; △, Krishnakumar and Srivastava, [52]; ▲, Ma et al., [97]; ○, McCallion et al., [42], —■—, Syage [41]; □, Straub et al., [103]; ×, Sorokin et al., [86]. Semiempirical values: ● de Heer et al., [55]; —– —, Lennon et al., [90] ——, Brusa et al., [17] ; –, Phelps et al. [100]; ●—●, this paper. Data compiled by the author.

Nagy et al. [96] have measured the absolute total cross sections in the relatively higher range of 0.5 keV-5 keV range by the a beam-static-gas configuration method and just three values (500, 700 and 1000 eV) are available in the range of our interest. A special feature of the setup used by Nagy et al. [96] is that the target gas is introduced into the source volume by two wide tubes and not through a collimated structure. Further the collision cell is divided into two interconnected parts, to ensure homogeneity of the target gas number density.

The measurements of Wetzel et al. [50] of the partial ionization coefficients in a crossed beam apparatus cover the energy range of onset- 200 eV and have a stated overall accuracy of 15%. The results of Stephan et al. [87] agree very well with the results of Wetzel et al. [50] and therefore not shown. The partial cross sections given by Wetzel have been converted to gross cross sections by the present author and are shown in Figure 10. The double hump observed in the cross section of argon^{3+} is interesting; the first hump occurs at an energy of 180 eV and it is due to

direct multiple ionization. The second hump is much broader and has onset energy of 250 eV. The second hump is due to the Auger process (Krishnakumar and Srivastava [52]). In this process an inner shell electron is ionized by the impacting electron and an outer electron, in transferring into the vacancy, gives the transition energy to another outer electron. If this energy is high enough the outer electron is ejected, thus leaving the atom ionized to one higher energy level (Kieffer and Dunn [84]).

Krishnakumar and Srivastava [52] have measured the partial ionization cross sections in rare gases from threshold to 1000 eV using a pulsed electron beam and ion extraction technique. A quadrupole mass spectrometer is used to collect charged particles and they have demonstrated that failure to correct for ion transmission losses and to optimize ion extraction efficiency can lead to considerable errors in the measured cross sections [97]. They normalized their relative data with the results of Rapp and Englander-Golden [84] for energies below the production of doubly charged ions. Using the relative flow technique the absolute cross sections of the multiply ionized species are determined. The total cross section is obtained by summation of the individual cross sections by proper weighting of the individual partial cross sections. A notable feature of the results obtained is that partial cross sections are obtained in all the rare gases, up to 1000 eV electron energy, in the same setup.

Ma et al. [97] have studied the absolute partial cross sections in argon, for three ionization levels using an electron impact spectrometer that uses a pulsed electron source and time of flight detection of electrons and ions. The time of flight method is thought to overcome the serious transmission losses in electrostatic analyzers and mass spectrometers. The range of electron energies is onset-500 eV and absolute partial cross sections up to triply charged ions are measured. The absolute total cross section shown in Figure 11 is computed by the present author from their tabulated absolute partial cross sections. These measurements were revised by Bruce and Bonham [98], upwards by about 15%.

McCallion et al. [42] have extended the time of flight technique to measure partial ionization cross sections, for five times charged ions, from onset energy up to 5300 eV. The absolute total cross section shown in Figure 11 is computed by the present author from their tabulated absolute partial cross sections. Syage's measurements [41] of partial cross sections are notable for the closely spaced intervals of the electron impact energy.

Sorokin et al. [86] have determined the absolute total electron impact ionization cross sections by measuring the total ion yield for both electron and photon impact ionization, in the range of electron energy of 140-4000 eV. The gas pressures are in the range of 0.2–1 mPa. Using the known photoionization cross sections and the ratios of ion yields, the electron ionization cross sections are determined.

Kobayashi et al. [99] have measured the ratio of partial ionization cross section to the total ionization cross section in the energy range covering threshold to 1000 eV. For singly charged ions the authors claim good agreement with other reported data.

We shall now consider the semi empirical values and equations that are useful for modelers and for evaluating the total ionization cross sections at any desired electron impact energy. de Heer et al. [55] have provided the total ionization cross sections in the range of 20–4000 eV using the sum rules and the peak of the cross section is 2.95×10^{-20} m^2 obtaining at 90 eV electron impact energy. Their data are in very good agreement with the data of Krishnakumar and Srivastava [52] above 100 eV. Lennon et al. [89] and Märk [88] have proposed a semi empirical equation of the form

$$Q_i = \frac{1}{\epsilon\epsilon_i}\left[A\ln\left(\frac{\epsilon}{\epsilon_i}\right) + \sum_{j=1}^{N} B_j\left(1-\frac{\epsilon_i}{\epsilon}\right)\right] \qquad (23)$$

where A and B are coefficients given in Table 7, ϵ the electron energy, ϵ_i the ionization energy and N the number of terms in the summation term. The advantage of this equation is that it can also be used to calculate the partial ionization cross sections in addition to the first ionization cross section. The calculated values of the total ionization cross sections in argon, using the coefficients given Table 8, are shown in Figure 11, with selected measured data. While the shape of the total ionization cross sections curve agrees well the agreement between measured and calculated data is improved by modifying equa-

Table 7. Parameters of Brusa et. al. [55] to calculate ionization cross sections in rare gases. n is the number of points used to extract the parameters. Reproduced with the permission of Zeit. Phys. D.

Parameter	Gas				
	Ar	He	Ne	Kr	Xe
n	52	50	50	52	54
Energy range (eV)	ϵ_i-5000	ϵ_i-5000	ϵ_i-5000	ϵ_i-5000	ϵ_i –5000
L (10^{-20} m^2)	78.76	2000	7.92	33.76	1000
M	18.62	70.9	7.04	15.93	53.79
N (10^{-20} m^2)	25.66	–	–	14.45	109.6
P (keV)	8.42×10^{-3}	1.49×10^{-3}	2.16×10^{-3}	1.26×10^{-3}	3.58×10^{-3}
ϵ_i (eV)	15.759	24.587	21.584	13.999	12.130

Table 8. Constants for using equation (24). A and B_j, taken from Lennon [89], in units of 10^{-23} eV^2m^2. $f(\epsilon)$ is evaluated by the author.

	Species		
Constant	Ar^+	Ar^{2+}	Ar^{3+}
A	2.532	2.086	1.170
B_1	−2.672	1.077	0.843
B_2	2.543	−2.172	−2.877
B_3	−0.769	0.809	1.958
B_4	0.008	–	–
B_5	0.006	–	–
$f(\epsilon)$	$0.4045\ \epsilon^{0.1844}$	0.0426	0.1333

tion (23) as

$$Q_i = \frac{f(\epsilon)}{\epsilon\epsilon_i}\left[A\ln\left(\frac{\epsilon}{\epsilon_i}\right) + \sum_{j=1}^{N} B_j\left(1-\frac{\epsilon_i}{\epsilon}\right)\right] \qquad (24)$$

where $f(\epsilon)$ is a correction function or constant. Brusa et al. [17] also provide a semiempirical equation for the total ionization cross section by using the data of Krishnakumar and Srivastava [52] and de Heer et al. [55]

$$Q_i = \left(\frac{L}{m+x}+\frac{N}{x}\right)\left(\frac{y-1}{x+1}\right)^{1.5} \times\left[1+\frac{2}{3}\left(1-\frac{1}{2x}\right)\ln\left\{2.7+(x-1)^{0.5}\right\}\right] \qquad (25)$$

where L, M, N and P are the four free parameters (Table 6) determined by the best fitting procedure, $y = \epsilon/\epsilon_i$ and $x = \epsilon/P$, ϵ_i the ionization potential and ϵ the electron energy.

Total ionization cross sections in argon calculated according to equation (25) are also shown in Figure 11. The shape of the curve is reproduced remarkably well and a particular advantage of this formula is that the total ionization cross sections at the onset give relatively more accurate total ionization cross sections. A more recent equation for the total ionization cross section is given by Phelps and Petrović [100, 101], for modeling cold cathode discharges,

$$Q_i(\epsilon) = 970\left[\frac{(\epsilon-15.8)}{(70+\epsilon)^2}\right] + 0.06(\epsilon-15.8)^2\exp\left(\frac{-\epsilon}{9}\right) \qquad (26)$$

A special feature of their modeling is that fast-atom interactions, which are generated by symmetric charge transfer collisions of Ar^+ with Ar, are considered for the first time in a cold-cathode discharge. The calculated values according to equation (26) are also in very good agreement as shown in Figure 11 and will be further commented upon with reference to Figure 13.

The partial ionization cross sections shown in Figure 12 cover the period from 1980. There are essentially three different types of data that have been reported; the relative partial cross section functions, absolute partial cross section functions and ratios of partial cross sections. The agreement between various measurements and with the semi empirical equation is poorer than in the case of the total ionization cross sections.

The measurements of Stephan et al. [87] using mass spectrometer belongs to the category of determination of relative partial ionization cross sections. Absolute total cross sections were obtained by normalization to the data of Rapp and Golden-Englander [84]. They observed a structure (also confirmed by Wetzel et al., [50]) around 50 eV for Ar^+ in the shape of a very low second maximum, possibly due to autoionization according to the process, $Ar + e \rightarrow Ar^+ + 3e$. In this process excitation from an inner orbital (3S) electron to ^1D and ^1S states of highly excited neutral Ar which autoionize into the adjacent Ar^+ continuum. Further, these authors did not find any peculiarity in the cross section for Ar^{3+}, because of their energy limitation to 180 eV, though the Auger process previously explained, has been observed by other groups for electron energies greater than about 250 eV.

Table 9. Authors and energy range within ±5% of the cross sections due to Rapp and Englander-Golden [84].

Authors	Energy range (eV)	Reference number
De Heer et al. (1979)	20–500	[55]
Stephan et al. (1980)	20–180	[87]
Wetzel et al. (1987)	18, 19, 25–75	[50]
Krishnakumar and Srivastava (1988)	30–650	[52]
Ma et al. (1991)	20–500	[87]
McCallion et al. (1992)	18, 57–1000	[42]
Syage (1992)	18, 24–660	[41]
Straub et al. (1995)	25, 100–1000	[103]
Brusa et al. (1996)	25–100	[17]
Phelps and Petrović (1999)	18.5–750	[100]
Sorokin et al. (2000)	140–1000[1]	[86]
Kobayashi et al. (2002)	16–1000[2]	[99]
Raju	30–90, 300–600	This paper

1. Multiply by 1.1
2. Multiply by 1.05

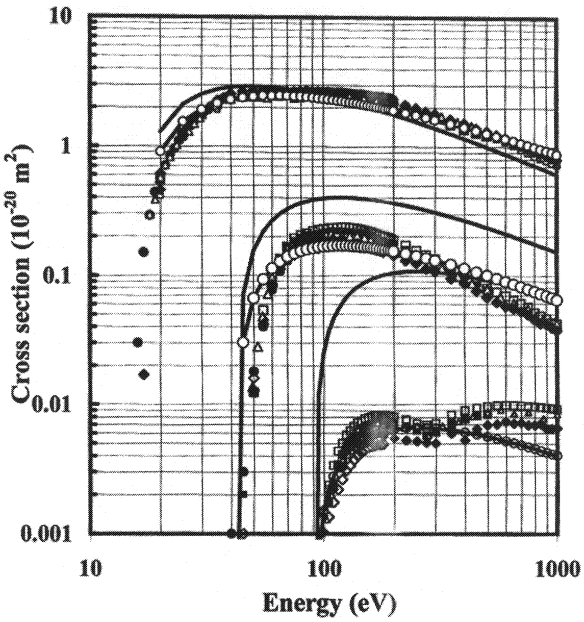

Figure 12. Partial ionization cross sections in argon. ◇, Stephan et al. [87]; ●, Wetzel et al. [50]; □, Krishnakumar et al. [52]; ■, Ma et al. [97]; △, McCallion et al. [42]; ♦, Straub et al. [103]; ——, Lennon et al. [89]; —□, Kobayashi et al., [99]; ○—○ This paper. The results of Mathur and Badrinath [53] are not shown.

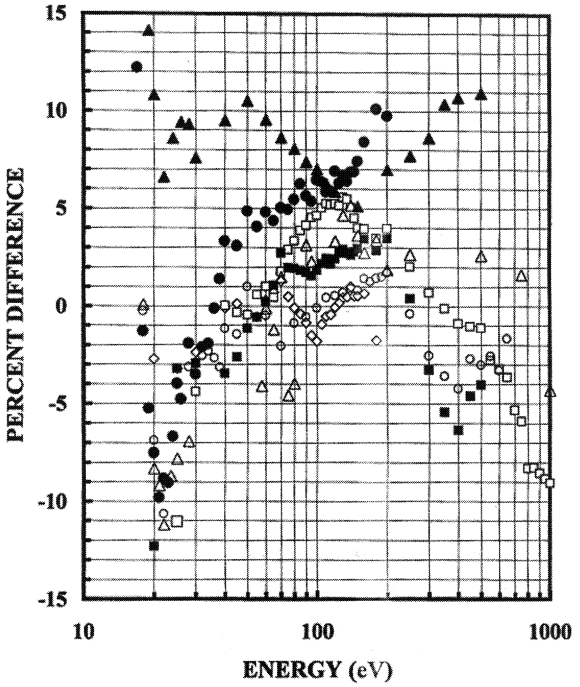

Figure 13. Comparison of total ionization cross sections in argon. Percent difference is calculated with respect to the tabulated values of Rapp and Englander-Golden [84] fpr overlapping energy values. ▲, Fletcher and Cowling [102]; ◇, Stephan et al. [87]; ●, Wetzel et al. [50]; □, Krishnakumar and Srivastava [52]; ■, Ma et al. [97]; ○, Syage [41]; △, McCallion et al. [42]. Data compiled by the author.

Figures 13 and 14 show a comparison of the measured absolute total cross sections by selected authors. The comparison has been made by arbitrarily choosing the data of

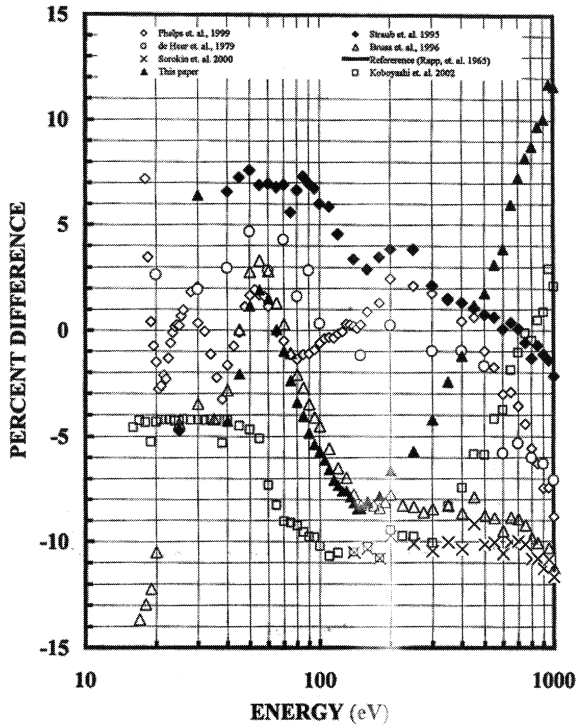

Figure 14. Comparison of total ionization cross sections in argon (continued). Percent difference is calculated with respect to the tabulated values of Rapp and Englander-Golden [84]. ♦, Straub et al. [103]; ×, Sorokin et al. [86]; Semiempirical values and equations: ○, de Heer et al. [55]; △, Brusa et al. [17]; ◇, Phelps and Petrović [100]; ▲, this paper, equation (24). Data calculated according to equation (23) are not shown as they fall outside the band of $\pm 15\%$.

Rapp and Englander-Golden [85] as reference, due to the reason that several modelers have demonstrated that the cross sections are reliable within a stated accuracy of 7%. At the onset energy there is considerable noise and meaningful comparison can be made only at energies greater than about 20 eV. Fletcher and Cowling [102] using the same technique as Rapp and Englander-Golden [84], obtained values that are higher by $5-14\%$.

The results of Stephan et al. [87] agree well, within $\sim$ 3%. The fast-atom beam method of Wetzel et al. [50] fall within $\pm 5\%$ for electron energies lower than 100 eV. The results of Krishnakumar and Srivastava [52] also lie within a $\pm$ 5% band except at energies greater than 800 eV. The results of Wetzel et al. [50] are about 6% higher than those of Krishnakumar and Srivastava [52].

The measured values of Ma et al. [97], McCallion et al. [42], Syage [41] and Straub et al. [103], all using the time of flight spectrometer are within the band of $\pm 5\%$. It is noted that Syage [41] constructed the curve of Ar^+ ionization cross sections by averaging the same results of Stephan et al. [87], Wetzel et al. [50], Krishnakumar and Srivastava [52] and Ma et al. [97]. This reference curve was then used to obtain partial ionization cross sections in Ar, Kr and Xe. The data obtained are closely spaced in

the energy scale up to 660 eV and extends the measurements to five times charged ions. More recent measurements of Sorokin et al. [86], employing the measurements of the ratios of photoelectron ionization to electron impact ionization are uniformly 10% lower over the range covered by them, 140–4000 eV. If one attributes the differences to the normalization process then the agreement of absolute total ionization cross sections between Sorokin et al. [86] and, Rapp and Englander-Golden [84] is within $\pm 1\%$.

There is considerably more disagreement in the partial ionization cross sections reported by several groups. Figure 15 shows the ratios of Ar^+/Ar(total), Ar^{2+}/Ar(total), and Ar^{3+}/Ar(total), as a function of electron energy; this ratio is chosen to avoid the need for choosing a reference. While there is very good agreement between various measurements for the ratio Ar^+/Ar(total), the remaining two ratios show considerable disagreement, sometimes by as much as a factor of two. The main reason is due to the differences in the partial ionization cross sections.

Table 8 shows the range of electron impact energies that fall within a band of $\pm 5\%$ of the cross sections due to Rapp and Englander-Golden [84] with appropriate references.

9 THE SIGMA RULE

The sigma rule, also called as the sum check provides a method of judging systematic differences, at least partially, that may exist in several sets of data carried out in different laboratories. The method is to add up the partial cross sections and compare it with the measured total cross sections. Such a check also helps in choosing a set of cross sections for modeling and determine the gaps in energy where more accurate experimentation is desirable. Zecca et al. [10] have carried out this kind of analysis at selected electron energies.

Table 10 and Figure 16 show the quality of the agreement over the energy range 12–1000 eV. Below the first excitation level the total scattering cross section is the same as the elastic collision cross section. At very low energies there are relatively few measurements of the total cross section; the data of Ferch et al. [37] covers the range 0.08–0.11 eV. The energy range of 0.12–10 eV is covered by Buckman et al. [38]. The notable resonance studies of Zubek et al. [104] cover the range of 100°–180° only. The inelastic collision cross section is composed of total excitation and ionization cross sections. Mason and Newell [39] have measured the total metastable cross sections in the range of 12–140 eV and Tsurubuchi et al. [81] have measured the lowest resonance cross sections. The sum of these two cross sections are taken as the total excitation cross sections, on the reasonable assumption that the total metastable cross sections above 140 eV make about 1% contribution (Figure 10).

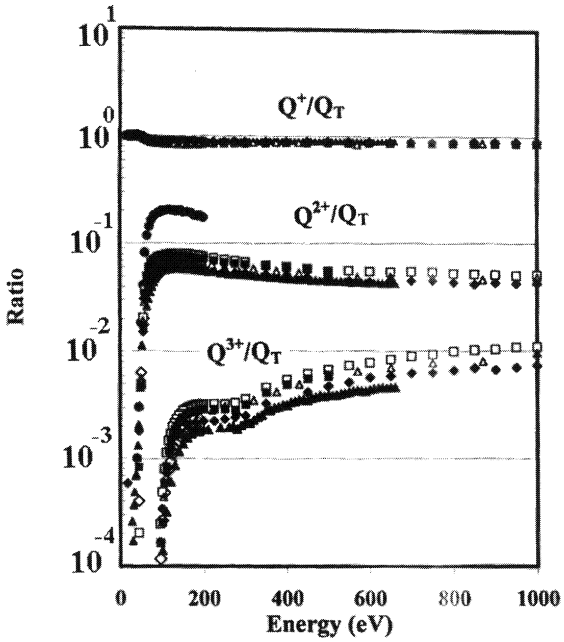

Figure 15. Ratios of partial cross sections to total ionization cross sections in argon. ◇, Stephan et al. [87]; ●, Wetzel et al. [50]; □, Krishnakumar and Srivastava [52]; ■, Ma et. al. [97]; ▲, Syage [41]; △, McCallion et al. [42]; ♦, Straub et al. [103]. Data compiled by the author.

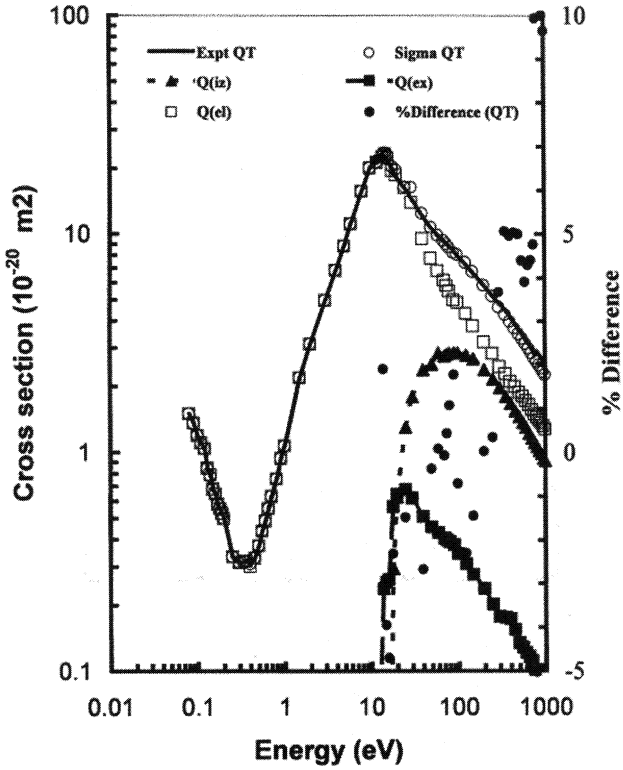

Figure 16. Verification of sigma rule and recommended cross sections. ——, experimental Q_T; ○, sigma Q_T-sum of cross sections from table 10; ●, percent difference between the two (right ordinate). Positive values mean that the experimental data are higher. □, Q_{el}; —■—, Q_{ex}; –▲–, Q_{iz}; from Table 10.

Table 10. Comparison of sigma rule and measured Q_T.

Energy	Qel	Qex	Qi	sigma(Q_T)	Q_T(Measured)	DIFFERENCE
	$10^{-20}(m^2)$	$10^{-20}(m^2)$	$10^{-20}(m^2)$	$10^{-20}(m^2)$	$10^{-20}(m^2)$	%
0.08	1.50[F,85]			1.5	1.50[F,85]	
0.1	1.19[F,85]			1.19	1.19[F,85]	
0.2	0.50[B,86]			0.5	0.50[B,86]	
0.5	0.374[B,86]			0.374	0.374[B,86]	
1	1.07[B,86]			1.07	1.07[B,86]	
5	8.81[B,86]			8.81	8.81[B,86]	
10	20.06[B,86]	**T+M**		20.06	20.06[B,86]	
12	21.25(I)[F89]	0.045(I)		21.31	22.84[B,86]	6.699
14	22.56(I)[F,89]	0.237		22.797	23.24[B,86]	1.906
15	23.22[F,89]	0.254	**R,65**	23.474	22.58(I)[B,86]	−3.959
16	22.30(I)[F,89]	0.262	0.02	22.963	21.93[B,86]	−4.710
18	19.52(I)[F,89]	0.565	0.294	20.433	19.97[B,86]	−2.318
20	18.60[F,89]	0.643	0.627	19.738	18.30[B,86]	−7.858
25	16.27[d,79]	0.676	1.302	16.45	16.21[N,85]	−1.481
30	13.94[d,79]	0.619	1.803	16.362	14.52[N,85]	−12.686
40	9.51[d,79]	0.511	2.393	12.414	12.09[N,85]	−2.680
50	7.74[d,79]	0.457	2.533	10.73	10.69[N,85]	−0.374
70	6.15[d,79]	0.406	2.771	9.327	9.320[N,85]	−0.075
90	5.00[d,79]	0.378	2.859	8.237	8.386[N,85]	1.777
100	4.86[d,79]	0.344	2.850	8.054	7.997[N,85]	−0.713
150	3.79(I)[d,79]	0.275	2.683	6.748	6.652[N,85]	−1.443
200	3.2[d,79]	0.237	2.393	5.83	5.831[N,85]	0.017
250	2.833(I)[d,79]	0.201	2.173	5.207	5.225[N,85]	0.344
300	2.466[d,79]	0.177	1.979	4.622	4.798[N,85]	3.668
350	2.290(I)[d,79]	0.175(I)	1.812	4.277	4.505[W,85]	5.061
400	2.115[d,79]	0.173	1.68	3.968	4.175[W,85]	4.958
450	2.0(I)[d,79]	0.154(I)	1.548	3.702	3.898[W,85]	5.028
500	1.885	0.134	1.46	3.479	3.662[W,85]	4.997
550	1.806(I)	0.128(I)	1.372	3.306	3.458[W,85]	4.396
600	1.728	0.121	1.302	3.151	3.279[W,85]	3.904
650	1.649(I)	0.116(I)	1.223	2.988	3.122[W,85]	4.292
700	1.571	0.111	1.161	2.843	2.974[W,85]	4.405
750	1.492(I)	0.101(I)	1.108	2.701	2.836[W,85]	4.760
800	1.448(I)	0.091	1.064	2.603	2.89[N,82]	9.931
850	1.405(I)	0.087(I)	1.02	2.512	2.795[N,82]	10.125
900	1.361	0.083	0.985	2.429	2.70[N,82]	10.037
1000	1.274	0.079	0.915	2.268	2.51[N,82]	9.641

I means interpolated
T+ M means Tsurubuchi et al. [81] + Mason and Newell [39]
R,65 means Rapp and Englander-Golden [85]
d,79 means de Heer et al. [55]
F,85 means Ferch et al. [37]
B,86 means Buckman and Lohmann [38]
W,85 means Wagenaar and de Heer, [34]
N, 82 means Nogueira et al. [57].

The data of de Heer et al. [55] are consistent up to 1000 eV. Alternately, the empirical formula of Zecca et. al. [10] up to 1000 eV is also satisfactory. In the high energy range, $>$ 750 eV, the measured total cross section of Noguiera et al. [57] joins smoothly to the data of Wagenaar et al. [34]. It is noted that Noguiera et al. [57] have provided two sets of data for the total scattering cross section; the measured cross sections and those with a theoretical correction applied for the small angle scattered electrons, $\sim$ 3−6%. Since the uncorrected values give better agreement for the sigma check it is possible that Noguiera et al. [57] have over corrected their values.

The elastic collision cross sections show the greatest differences between various measurements and very few measurements are carried out above 20 eV since 1980. The measurements of Srivastava et al. [60] are rather too low and the more recent measurements of Gibson et al. [49] are limited to 10 eV electron energy. Therefore one has to look for theoretical calculations or experiments prior to 1980 in measured ones and those to which a theoretical correction is applied to account for forward low angle scattering.

It is concluded that the sigma rule applies to argon quite well in the energy range studied and the cross sections shown in Table 10 may be regarded as a recommended set.

ACKNOWLEDGMENTS

The author wishes to thank the Natural Sciences and Engineering Research Council of Canada for a grant to carry out the work. Thanks are due to Dr. A. Kobayashi for providing tabulated values of their results and Dr. L. Pitchford for providing most recent momentum transfer

data shown in Figure 1. Thanks are also due to Dr. J.W. McConkey for providing reference [10] and for helpful advice. The help of the referees in improving the manuscript is acknowledged.

Note: Swarm coefficients have been calculated using the two term Boltzmann code of Bolsig [83], the momentum transfer cross sections of [60] and cross sections of Table 10. They will be published elsewhere.

REFERENCES

[1] J. M. Meek and J. D. Craggs, *Electrical Breakdown in Gases*, John Wiley & Sons, New York, 1979; T. D. Märk and G. H. Dunn. (eds.): *Electron Impact Ionization*, Wien, New York: Springer, 1985.

[2] C. Ramsauer, "Über den wirkungsquerschnitt der Gasmoleküle gegenüber lengsomen Electronen. I-Fortsetzung, Ann. Phys. (Lpz), Vol. 66, pp. 546–561, 1921.

[3] R. E. Brode, Phys. Rev., "The Absorption Coefficient for Slow Electrons in Gases", Vol. 25, pp. 636–644, 1925; Rev. Mod. Phys.,Vol. 5, pp. 257–292, 1933.

[4] H. S. W. Massey and E. H. S. Burhop, *Electronic and Ionic Impact Phenomena*, Oxford University Press, Oxford, chapters 1-4, 1952.

[5] B. Bederson and L. J. Kieffer, "Total Electron-Atom Collision Cross Sections at Low Energies—A Critical Review", Rev. Mod. Phys., Vol. 43, 601-640, 1971.

[6] B. H. Bransden and M. R. C. McDowell, "Electron Scattering by Atoms at Intermediate Energies", Phys. Rep., Vol. 46, pp. 249–394, 1978.

[7] E. W. McDaniel, *Collision Phenomena in Ionized Gases*, John Wiley & Sons, New York, 1964.

[8] J. B. Hasted, *Physics of Atomic Collisions*, Amer. Elsevier Pub. Co., New York, (II ed.), 1972.

[9] S. Trajmar and J. W. McConkey, "Benchmark Measurements of Cross Sections for Electron Collisions: Analysis of Scattered Electrons", Advances in Atomic, Molecular, and Optical Physics, Bederson and Walther (eds.), Vol. 33, pp. 63–89, 1994.

[10] A. Zecca, G. P. Karwasz and R. S. Brusa, "One Century of Experiments on Electron-Atom and Molecule Scattering : A Critical Review of Integral Cross Sections I. Atoms and Diatomic Molecules", La Rivista del Nuovo Cimento, Vol. 19, pp. 1-146, 1996.

[11] A. Chutjian and D. C. Cartwright, "Electron – Impact Excitation of Electronic States in Argon at Incident Energies Between 16 and 100 eV", Phys. Rev. A, Vol. 23, pp. 2178–2193, 1981.

[12] C. Ramsauer and R. Kollath, "Űber den Wirkungsquerschnitt der Edelgasmolküle gegenüber Elektronenunterhalb 1 Volt", Ann. Phys. Lpz., Vol. 3, pp. 536–564, 1929.

[13] C. Ramsauer and R. Kollath, "Die Winkelverteilung bei der Streuung langsammer Elektronen an Gasmolekülen", Ann. Phys. Lpz., Vol. 12, pp. 529–561, 1932.

[14] J. S. Townsend and V. A. Bailey, Phil. Mag., "The Motion of Electrons in Argon and in Hydrogen", Vol. 44, pp. 1033–1052, 1922.

[15] J. S. Townsend and V. A. Bailey, Phil. Mag., "The Motion of Electrons in Gases", Vol. 46, pp. 661–675, 1923.

[16] von H. Faxen and J. Holtsmark, Z. Phys., "Beitrag zur Theorie des Durchganges langsamer Elektronen durch Gase", Vol. 45, pp. 307–324, 1929.

[17] R. S. Brusa, G. P. Karwasz and A. Zecca, "Analytical Partitioning of Total Cross Sections for Electron Scattering on Noble Gases", Z. Phys. D, Vol. 38, pp. 279–287, 1996.

[18] A. Zecca, G. P. Karwasz and R. S. Brusa, J. Phys. B: At. Mol. Opt. Phys., "Electron Scattering by Ne, Ar and Kr at Intermediate and High Energies, 0.5-10 keV", Vol. 33, pp. 843–845, 2000.

[19] M. Inokuti, M. Kimura, M. A. Dillon, and I. Shimamura, "Analytic Representation of Cross Section Data", Advances in Atomic, Molecular, and Optical Physics, Bederson and Walther (eds.), Vol. 33, pp. 215–251, 1994.

[20] T. F. O'Malley, L. Spruch, and L. Rosenberg, "Modification of Effective Range Theory in the Presence of a Long Range (r^{-4}) Potential", Math. Phys., Vol. 2, pp. 491–498, 1961.

[21] M. Inokuti and M. R. C. McDowell, "Elastic Scattering of Fast Electrons by Atoms I. Helium to Neon", J. Phys. B: At. Mol. Phys., Vol. 7, 23822395, 1974.

[22] A. Zecca, G. P. Karwasz, R. S. Brusa, "Total Cross Section Measurements for Electron Scattering by NH_3, SiH_4, and H_2S in the Intermediate Range", Phys. Rev. A, Vol. 45, pp. 2777–2783, 1992.

[23] A. Zecca, G. P. Karwasz, R. S. Brusa, "Absolute Total Cross Section Measurements for Intermediate Energy Electron Scattering on CF_4, $CClF_3$, CCl_2F_2, CCl_3F and CCl_4", Phys. Rev. A, Vol. 46, pp. 3877–3882, 1992.

[24] A. Zecca, J. C. Nogueira, G. P. Karwasz, R. S. Brusa, "Total Cross Sections for Electron Scattering on NO_2, OCS, SO_2 at Intermediate Energies", J. Phys. B: At. Mol. Opt. Phys., Vol. 28, pp. 477–486, 1995.

[25] N. H. March, A. Zecca, G. P. Karwasz, "Phenomenology and Scaling of Electron Scattering Cross Sections from Almost Spherical Molecules Over a Wide Energy Range", Z. Phys. D., Vol. 32, pp. 93-100, 1994.

[26] G. Garcia, F. Arqueros and J. Campos, (a) "Total Cross Sections for Electron Scattering from Ne, Ar and Kr in the Energy Range 700-6000 eV", J. Phys. B: At. Mol. Phys., Vol. 19, pp. 3777–3785, 1986; (b) G. Garcia, M. Roteta, F. Manero, F. Blanco, and A. Williart, "Electron Scattering by Ne, Ar, Kr, at Intermediate and High Energies, 0.5-10 keV", J. Phys. B: At. Mol. Opt. Phys., Vol. 32, 1783-, 1999.

[27] D. E. Golden and H. W. Bandel, "Low-Energy e^-Ar Total Scattering Cross Sections: The Ramsauer-Townsend Effect", Phys. Rev., Vol. 149, pp. 58–59, 1966; Absolute Total Electron-Helium-Atom Scattering Cross Sections for Low Energy Electron Energies", Phys. Rev., A Vol. 138, pp. 14–21, 1965.

[28] G. Dalba, P. Fornasini, I. Lazzizzera, G. Ranieri, A. Zecca, "Absolute Total Cross Section Measurements for Intermediate Energy Electron Scattering I. He", J. Phys. B: At. Mol. Phys., Vol. 12, pp. 3787–3795, 1979.

[29] G. Dalba, P. Fornasini, R. Grizenti, I. Lazzizzera, G. Ranieri, A. Zecca, "Ramsauer Type Apparatus for Absolute Total Cross Section Measurements at Intermediate Energy", Rev. Sci. Inst. Vol. 52, pp. 979-983, 1981.

[30] A. Zecca, S. Oss, G. Karwasz, R. Grisenti, R. S. Brusa, "Absolute Total Cross Section Measurements for Intermediate Energy Electron Scattering: III. Ne and Ar", J. Phys. B: At. Mol. Phys., Vol. 20, pp. 5157–5164, 1987.

[31] A. Zecca, G. Karwasz, R.S. Brusa, R. Grisenti, "Absolute Total Cross Section Measurements for Intermediate-Energy Electron Scattering: IV. Kr and Xe", J. Phys. B. At. Mol. Opt. Phys., Vol. 24, pp. 2737–2746, 1991.

[32] J. W. McConkey and F. G. Donaldson, "Excitation of the Resonance Lines of Ar by Electrons", Can. J. Phys., Vol. 51, pp. 914–921, 1973.

[33] J. C. Nickel, K. Imre, D. F. Register, S. Trajmar, "Total Electron Scattering Cross Sections: I. He, Ne, Ar, Xe", J. Phys. B: At. Mol. Phys., Vol. 18, pp. 125–133, 1985.

[34] R. W. Wagenaar and F. J. de Heer, "Total Cross Sections for Electron Scattering from Ar, Kr and Xe", J. Phys. B: At. Mol. Phys., Vol. 18, pp. 2021–2036, 1985. Also see K. Jost, P. G. F. Bisling, F. Eschen, M. Felsmann and L. Walther, Proc. 13th Inter. Conf. on the Physics of Electronic Atomic Collisions, Berlin, Ed: J. Eichler, et al., (Amsterdam, North Holland) p. 91, 1983, cited by R. W. Wagenaar and F. J. de Heer, et [66]. Tabulated values above 7.5 eV are given in the latter reference. The lower range of 0.05 eV is obtained from Nickel et. al. [33].

[35] R. W. Wagenaar, A. de Boer, T. van Tubergen, J. Los and F. J. de Heer, "Absolute Differential Cross Sections for Elastic Scattering of Electrons over Small Angles from Noble Gas Atoms", J. Phys. B: At. Mol. Phys., Vol. 19, pp. 3121–3143, 1986.

[36] R. E. Kennerly and R. A. Bonham, "Electron-Helium Absolute Total Scattering Cross Sections from 0.5-50 eV", Phys. Rev. A, Vol. 17, pp. 1844–1854, 1978.

[37] J. Ferch, B. Granitza, C. Masche, and W. Raith, "Electron-Argon Total Cross Section Measurements at Low Energies by Time-of-Flight Spectroscopy", J. Phys. B: At. Mol. Phys., Vol. 18, pp. 967–983, 1985.

[38] S. J. Buckman, B. Lohmann, "Low-Energy Total Cross Section Measurements for Electron Scattering from Helium and Argon", J. Phys. B: At. Mol. Phys., Vol. 19, pp. 2547–2563, 1986.

[39] N. J. Mason, W. R. Newell, "Total Cross Sections for Metastable Excitation in the Rare Gases", J. Phys. B: At. Mol. Phys., Vol. 20, pp. 1357–1377, 1987.

[40] J. E. Furst, D. E. Golden, M. Mahgerefteh, J. Zhou, and D. Mueller, "Absolute Low Energy e^--Ar Scattering Cross Sections, Phys. Rev. A, Vol. 40, pp. 5592–5600, 1989.

[41] J. A. Syage, "Electron-Impact Cross Sections for Multiple Ionization of Kr and Xe", Phys. Rev. A, Vol. 46, pp. 5666–5679, 1992.

[42] P. McCallion, M. B. Shah and H. B. Gilbody, "A Crossed Beam Study of the Multiple Ionization of Argon by Electron Impact", J. Phys. B: At. Mol. Phys., Vol. 25, pp. 1061–1071, 1992.

[43] K. R. Asmis and M. Allan, "Measurement of Absolute Differential Cross Sections for the Excitation of the $n = 2$ States of Helium at 0° and 180°", J. Phys. B: At. Mol. Ipt. Phys., Vol. 30, pp. 1961–1974, 1997.

[44] D. Cubric, D. J. L. Mercer, J. M. Channing, G. C. King and F. H. Read, "A Study of Inelastic Scattering in He Covering the Complete Range from 0° to 180°", J. Phys. B: At. Mol. Opt. Phys., Vol. 32, pp. L45–L50, 1999.

[45] Z. Qing, M. J. M. Beerlage, and M. J. van der Wiel, "Angular Distributions of Electrons Elastically Scattered from Argon and Krypton at Energies Between 10 and 50 eV", Physica, Vol. 113C, pp. 225-236, 1982.

[46] D. F. Register and S. Trajmar, "Differential, Integral, and Momentum-Transfer Cross Sections for Elastic Electron Scattering by Neon: 5 to 500 eV", Phys. Rev. A, Vol. 29, pp. 1785–1792, 1984.

[47] I. Iga, L. Mu-Tao, J. C. Nogueira, and R. S. Barbieri, "Elastic Differential Cross Section Measurements for Electron Scattering from Ar and O_2 in the Intermediate Energy Ramge", J. Phys. B: At. Mol. Phys., Vol. 20, pp. 1095–1104, 1987.

[48] C. Szmytkowski, K. Maciag and G. Karwasz, "Absolute Electron-Scattering Total Cross Section Measurements for Noble Gas Atoms and Diatomic Molecules", Phys. Script., Vol. 54, pp. 271–280, 1996.

[49] J. C. Gibson, R. J. Gulley, J. P. Sullivan, S. J. Buckman, V. Chan and P. D. Burrow, "Elastic Electron Scattering from Argon at Low Incident Energies", J. Phys. B: At. Mol. Opt. Phys., Vol. 29, pp. 3177–3195, 1996.

[50] R. C. Wetzel, F.A. Baiocchi, T. R. Hayes, and R. S. Freund, "Absolute Cross Sections for Electron -Impact Ionization of the Rare Gas Atoms by the Fast-Neutral-Beam Method", Phys. Rev. A, Vol. 35, pp. 559–576, 1987.

[51] M. B. Shah, D. S. Elliot and H. B. Gilbody, "Pulsed Crossed-Beam Study of the Ionization of Atomic Hydrogen by Electron Impact", J. Phys. B: At. Mol. Phys., Vol. 20, pp. 3501–3514, 1987.

[52] E. Krishnakumar and S. K. Srivastava, "Ionization Cross Sections of Rare Gas Atoms by Electron Impact", J. Phys. B: At. Mol. Phys., Vol. 21, pp. 1055–1082, 1988.

[53] D. Mathur and C. Badrinathan, "Single and Multiple Ionization of Ar and Kr by Low Energy Electrons Impact Using a Crossed Beam Apparatus", Int. J. Mass. Spectr. Ion Proc., Vol. 57, pp. 167–178, 1984; "On the Ionization of Xenon by Electrons", Int. J. Mass. Spectr. Ion Proc., Vol. 68, pp. 9–14, 1986.

[54] A. A. Sorokin, L. A. Schmaenok, S. B. Bobashev, B. Möbus, M. Richter and G. Ulm, "Measurements of Electron-Impact Ionization Cross Sections of Argon, Krypton, and Xenon by Comparison with Photoionization", Phys. Rev. A, Vol. 61, 022723-1-11, 2000.

[55] F. J. de Heer, R. H. J. Jansen, and W. van der Kaay, "Total Cross Sections for Electron Scattering by Ne, Ar, Kr and Xe", J. Phys. B: At. Mol. Phys., Vol. 12, pp. 979–1002, 1979.

[56] W. E. Kauppila, T. S. Stein, J. H. Smart, M. S. Dababneh, Y. K. Ho, J. P. Downing, and V. Pol, Measurements of Total Scattering Cross Sections for Intermediate-Energy Positrons and Electrons Colliding with Helium, Neon and Argon", Phys. Rev. A, Vol. 24, pp. 725–742, 1981.

[57] J. C. Nogueira, Ione Iga, and Lee Mu-Tao, "Total Cross Sections for Electrons Scattered from Gases: 0.5-3.0 keV range on Ar", J. Phys. B: At. Mol. Phys., Vol. 15, pp. 2539–2549, 1982.

[58] R. W. Wagenaar, and F. J. de Heer, "Total Cross Sections for Electron Scattering from Ne, Ar, Kr and Xe", J. Phys. B: At. Mol. Phys., Vol. 13, pp. 3855–3866, 1980.

[59] K. P. Subramanian and V. Kumar, "Total Electron Scattering Cross Sections for Argon, Krypton and Xenon at Low Energies", J. Phys. B: At. Mol. Phys., Vol. 20, pp. 5505–5515, 1987.

[60] S. K. Srivastava, H. Tanaka, A. Chutjian and S. Trajmar, "Elastic Scattering of Intermediate-Energy Electrons by Argon", Phys. Rev. A, Vol. 23, pp. 2156–2166, 1981.

[61] J. L. Pack, R. E. Voshall and A. V. Phelps, "Longitudinal Electron Diffusion Coefficients in Gases: Noble Gases", J. Appl. Phys., Vol. 71, pp. 5363–5371, 1992.

[62] A. G. Engelhardt and A. V. Phelps, "Transport Coefficients and Cross Sections in Argon and Hydrogen-Argon Mixtures", Phys. Rev., Vol. A133, pp. 375–380, 1964. For a description of the method see Frost and Phelps, "Rotational Excitation and Momentum Transfer Cross Sections for Electrons in H_2 and N_2 from Transport Coefficients", Phys. Rev., Vol. 127, pp. 1621-1633, 1962.

[63] S. N. Nahar and J. M. Wadhera, "Elastic Scattering of Positrons and Electrons by Argon", Phys. Rev. A, Vol. 35, pp. 2051–2064, 1987.

[64] G. M. Webb, "The Elastic Scattering of Electrons in Argon and Krypton", Phys. Rev., Vol. 47, pp. 379–383, 1935.

[65] M. Weyherter, B. Barzick, A. Mann and F. Linder, "Measurements of Differential Cross Sections for e-Ar, Kr, Xe Scattering at E = 0.05-2 eV", Z. Phys. D., Vol. 7, pp. 333–347, 1988.

[66] M. Zubek, N. Gulley, G. C. King, and F. H. Read, "Measurements of Elastic Electron Scattering in the Backward Hemisphere", J. Phys. B: At. Mol. Opt., Vol. 29, pp. L239–L244, 1996.

[67] D. Cvejanović and A. Crowe, "Differential Cross Sections for Elastic Scattering of Electrons from Argon and Krypton as a Continuous Function of Energy", J. Phys. B: At. Mol. Opt. Phys., Vol. 30, pp. 2873–2887, 1997.

[68] J. F. Williams and B. A. Willis, "The Scattering of Electrons from Inert Gases-I. Absolute Differential Elastic Cross Sections for Argon Atoms", J. Phys. B: At. Mol. Phys., Vol. 8, pp. 1670–1682, 1975.

[69] J. F. Williams, "A Phaseshift Analysis of Experimental Angular Distributions of Electrons Elastically Scattered from He, Ne, and Ar over the Range 0.5 to 20 eV", J. Phys. B: At. Mol. Phys., Vol. 12, pp. 265–282, 1979.

[70] R. P. McEachran and A. D. Stauffer, "Elastic Scattering of Electrons from Neon and Argon, J. Phys. B: At. Mol. Phys., Vol. 16, pp. 4023–4038, 1983.

[71] R. Panajotović, D. Filipović, B. Marinković, V. Pejćev, M. Kurepa and L. Vušković, "Critical Minima in Elastic Electron Scattering by Argon", J. Phys. B: At. Mol. Phys., Vol. 30, pp. 5877-5894, 1997.

[72] J. E. Sienkiewicz, V. Konopińska, S. Telega and P. Syty, "Critical Minima in Elastic Electron Scattering from Argon", J. Phys. B: At. Mol. Op. Phys., Vol. 34, L409-, 2001.

[73] B. L. Moiseiwitsch and S. J. Smith, "Electron Impact Excitation of Atoms", Rev. Mod. Phys., Vol. 40, pp. 238–353, 1968.

[74] I. I. Fabrikant, O. B. Shpenik, A. V. Snegursky, and A. N. Zavilopulo, "Electron Impact Formation of Metastable Atoms", Phys. Rep., Vol. 159, pp. 1–97, 1988.

[75] D. W. O. Heddle and J. W. Gallagher, "Measurements of Elec-

tron Impact Optical Excitation Functions", Rev. Mod. Phys., Vol. 61, pp. 221–278, 1989.

[76] D. M. Filipović, B. P. Marinković, V. Pejčev and L. Vušković, "Electron-Impact Excitation of Argon: I. The 4s′ $[1/2]_1$, 4p $[1/2]_1$ and 4p′ $[1/2]_0$ States", J. Phys. B: At. Mol. Opt. Phys. Vol. 33, pp. 677-691, 2000.

[77] M. Hayashi. See also, K. Kosaki and M. Hayashi, Denkigakkai Zenkokutaikai Yokoshu (Prepr. Natl. Meet. Inst. Electr. Eng. Jpn.), (1992).

[78] A. R. Filippeli, C. C. Lin, L. W. Anderson, and J. W. McConkey, "Measuring Electron-Impact Excitation Cross Sections", Advances in Atomic, Molecular and Optical Physics, Vol. 33, pp. 2-54, 1994.

[79] J. E. Chilton, J. B. Boffard, R. S. Schaffe, and C. C. Lin, "Measurement of Electron-Impact Excitation into the $3p^5 4P$ levels of Argon using Fourier-Transform Spectroscopy", Phys. Rev. A, Vol. 57, pp. 267–277, 1998.

[80] A. A. Mityureva and V. V. Smirnov, "Excitation of Heavy Rare Gases to Metastable States by Electron Impact", J. Phys. B: At. Mol. Opt. Phys., Vol. 27, pp. 1869–1880, 1994.

[81] S. Tsurubuchi, T. Miyazaki, and K. Motohashi, "Electron-Impact Emission Cross Sections of Ar", J. Phys. B: At. Mol. Opt. Phys., Vol. 29, pp. 1785–1801, 1996.

[82] D. M. Filipović, B. P. Marinković, V. Pejčev and L. Vušković, "Electron-Impact Excitation of Argon: II. The lowest resonance 4s $[3/2]_1$ and Metastable 4s $[3/2]_2$ and 4s′ $[1/2]_0$ States", J. Phys. B: At. Mol. Opt. Phys., Vol. 33, pp. 2081–2094, 2000.

[83] L. C. Pitchford, Personal communication (2003). Also see A. Fiala, L. C. Pitchford and J. P. Boeuf, "Two-Dimensional Hybrid model of Low-Pressure Glow Discharges", Phys. Rev. E, Vol. 49, pp. 5607–5621, 1994.

[84] D. Rapp and P. Englander-Golden, "Total Cross Sections for Ionization and Attachment in Gases by Electron Impact. I. Positive Ionization", J. Chem. Phys., Vol. 13, pp. 1464–1479, 1965.

[85] L. J. Kieffer and G. H. Dunn, Rev. Mod. Phys., "Electron Impact Ionization Cross-Section Data for Atoms, Atomic Ions, and Diatomic Molecules: I. Experimental Data", Vol. 38, pp. 1–35, 1966.

[86] A. A. Sorokin, L. A. Schmaenok, S. B. Bobashev, B. Möbus, M. Richter, and G. Ulm, "Measurements of Electron-Impact Cross Sections of Argon, Krypton, and Xenon by comparison with Photoionization", Phys. Rev., Vol. 61, 022723-1-11, 2000.

[87] K. Stephan, H. Helm, and T. D. Märk "Mass Spectrometric Determination of Partial Electron Impact Ionization Cross Sections of He, Ne, Ar, and Kr from Threshold up to 180 eV", J. Chem. Phys., Vol. 73, pp. 3763-3778, 1980.

[88] T. D. Märk and G. H. Dunn (eds.): *Electron Impact Ionization*, Wien, New York: Springer, 1985.

[89] M. A. Lennon et. al., "Recommended Data on the Electron Impact Ionization of Atoms and Ions: Flourine to Nickel", J. Phys. Chem. Ref. Data, Vol. 17, pp. 1285–1363, 1988.

[90] R. K. Asundi and M. V. Kurepa, "Ionization Cross Sections in He, Ne, Kr, and Xe by Electron Impact", J. Electron. Control, Vol. 15, pp. 41–50, 1963.

[91] B. L. Schram, F.J. deHeer, F. J. van Der Wieland, J. Kistemaker, "Ionization Cross Sections for Electrons (0.6–20 keV) in Noble and Diatomic Gases", Physica, Vol. 31, pp. 94–112, 1965.

[92] B. L. Schram, J. H. Boerboom, and J. Kistemaker, "Partial Ionization Cross Sections of Noble Gases for Electrons with Energy 0.5–16 keV. I. Helium and Neon", Physica, Vol. 32, pp. 185–196, 1966.

[93] B. L. Schram, "Partial Ionization Cross Sections of Noble Gases for Electrons with Energy 0.5-18 keV", Physica, Vol. 32, pp. 197–208, 1966.

[94] B. L. Schram, H. R. Moustafa, H. R. Schutten, and F. J. de Heer, "Ionization Cross Sections for Electrons (100-600 eV) in Noble and Diatomic Gases", Physica, Vol. 32, pp. 734–740, 1966.

[95] J. Fletcher and I. R. Cowling, "Electron Impact Ionization of Neon and Argon", J. Phys. B: At. Mol. Phys., Vol. 6, pp. L258–L261, 1973.

[96] P. Nagy, A. Skutlartz and V. Schmidt, "Absolute Ionization Cross Sections for Electron Impact in Rare Gases", J. Phys. B: At. Mol. Phys., Vol. 13, pp. 1249–1267, 1980.

[97] C. Ma, C. R. Sporeleder and R. A. Bonham, "A Pulsed Electron Beam Time of Flight Apparatus for Measuring Absolute Electron Impact Ionization and Dissociative Ionization Cross Sections", Rev. Sci. Instr., Vol. 62, pp. 909–923, 1991.

[98] M. R. Bruce and R. A. Bonham, "Problems in the Measurement of the Ar^{+2}/Ar^{+} Partial Ionization Cross Section Ratio by use of the Pulsed Electron Beam Time of Flight Methos", Z. Phys. D, Vol. 24, pp. 149-154, 1992.

[99] A. Kobayashi, G. Fujiki, A. Okaji and T. Masuoka, "Ionization Cross Section Ratios of Rare-Gas Atoms (Ne, Ar, Kr and Xe) by Electron Impact from Threshold to 1 keV", J. Phys. B: At. Mol. Opt. Phys., Vol. 35, pp. 2087–2103, 2002.

[100] A. V. Phelps and Z. Lj. Petrović, "Cold-Cathode Discharges and Breakdown in Argon: Surface and Gas Phase Production of Secondary Electrons", Plasma Sources Sci. Tech., Vol. 8, pp. R21–R44, 1999.

[101] A. V. Phelps, C. H. Greene and J. P. Burke, "Collision Cross Sections for Argon Atoms with Argon Atoms for Energies from 0.01 eV to 10 keV", J. Phys. B: At. Mol. Opt. Phys., Vol. 33, pp. 2965–80, 2000.

[102] J. Fletcher and I. R. Cowling, "Electron Impact Ionization of Neon and Argon", J. Phys. B: At. Mol. Phys., Vol. 6, pp. L258–L261, 1973.

[103] H. C. Straub, P. Renault, B. G. Lindsay, K. A. Smith and R. F. Stubbings, "Absolute Partial and Total Cross Sections for Electron-Impact Ionization of Argon from Threshold to 1000 eV", Phys. Rev. A, Vol. 52, pp. 1115–1124, 1995.

[104] M. Zubek, B. Mielewska, J. Channing, G. C. King, and F. H. Read, "A Study of Resonance Structures in Elastic Electron Scattering from Helium, Neon, Argon, Krypton and Xenon over the Angular Range from 100° to 180°", J. Phys. B: At. Mol. Opt. Phys., Vol. 32, pp. 1351–1362, 1999.

Gorur G. Raju was born in 1937. He obtained the B.Eng. degree in electrical engineering from the University of Bangalore, India, and the Ph.D. degree from the university of Liverpool, U.K. He then worked in the research laboratories of Associated Electrical Industries, U.K. He joined the Department of HV Engineering, in Bangalore, and became its Head during 1975-1980. He joined the University of Windsor, Ontario, Canada in 1980 and became the Head of the Department of Electrical Engineering during 1989-1997 and 2000-2002. He is currently an Emeritus Professor at the University of Windsor. He has published over 100 research papers and two books. He is a registered Professional Engineer and Fellow of the Institute of Engineers, India.